Supporting Information

Bis-BN-Embedded [4]helicenes: Synthesis, Structures and Properties

Bingkang Liu,[a] Jiahao Cui,[b] Xiaoming Wu,[b] Jing Zhou,[c] Lei Zhang[d], Chenglong Li,[*a] and Xuguang Liu[*a]

[a] Tianjin Key Laboratory of Organic Solar Cells and Photochemical Conversion, School of Chemistry and Chemical Engineering, Tianjin University of Technology, Tianjin 300384, People's Republic of China.
[b] Key Laboratory of Display Materials and Photoelectric Devices (Ministry of Education), Tianjin Key Laboratory of Photoelectric Materials and Devices, National Demonstration Center for Experimental Function Materials Education, School of Materials Science and Engineering, Tianjin University of Technology, Tianjin 300384, People's Republic of China.
[c] College of Pharmacy, Shaanxi University of Traditional Chinese Medicine, Shaanxi 712046, People's Republic of China.
[d] School of Science, Tianjin Chengjian University, Tianjin 300384, People's Republic of China

Email:
Chenglong Li: chenglongli1991@email.tjut.edu.cn;
Xuguang Liu: xuguangliu@tjut.edu.cn

Contents:

1. General Materials and Methods

All oxygen- and moisture-sensitive manipulations were carried out under an inert atmosphere using either standard Schlenk techniques or a nitrogen-filled drybox. THF and toluene were purified by sodium absorption under argon. All other chemicals and solvents were purchased and used as received. Tetratriphenylphosphine palladium ($Pd(PPh_3)_4$), 1,4-dioxane, boron tribromide (BBr_3), 1,2,4-trichlorobenzene (1,2,4-TCB) (extra dry, with molecular sieves), triethylamine (TEA) (extra dry, with molecular sieves), methylmagnesium bromide (3.0 M in diethyl ether), phenylmagnesium bromide (1.0 M in THF) , trimethylsilylacetylene (TMSA), cuprous iodide (CuI), tetrabutylammonium bromide (n-Bu_4NBr), 2-aminophenylboronic acid and were purchased from Energy Chemical (Shanghai, China). 2-iodoaniline, N-bromosuccinimide (NBS), anhydrous aluminium chloride ($AlCl_3$), dichlorophenylborane ($PhBCl_2$), were purchased from Heowns Biochemical Technology Co., Ltd. (Tianjin, China). Mesitylmagnesium bromide (1.0 M solution in THF) was purchased from J&K Chemical (Beijing, China). Potassium carbonate (K_2CO_3), petroleum ether (PE), ethyl acetate (EA), dichloromethane (DCM), ethanol, methanol and THF were purchased from Hengshan Chemical (Tianjin, China). Toluene was purchased from Tianjin Chemical Reagent Company. And bromine was purchased from Damao Chemical Reagent Factory (Tianjin, China).

^1H NMR and ^{13}C NMR spectra were recorded on a Bruker AM-400 spectrometer. The reported chemical shifts were against TMS. ^{11}B spectra were recorded on a Bruker AM-400 spectrometer. The reported chemical shifts were against $BF_3 \cdot Et_2O$. HRMS were obtained on Waters Xevo Q-TOF MS with ESI resource. IR spectra were recorded on a Tensor 27 instrument with a Bruker OPTIK GmbH (Made in Germany) spectrometer.

IR spectra were recorded on a Tensor 27 instrument with a Bruker OPTIK GmbH (Made in Germany) spectrometer.

The absorption spectra of all compounds were measured by Thermo Scientific Evolution 201 spectrophotometer. Fluorescence measurements were carried out with an F-7000 fluorescence spectrophotometer. Fluorescence quantum yields were determined using the comparative method, 9,10-diphenylanthracene were referenced to cyclohexane (λ_{ex} = 340 nm, Φ_F = 0.93±0.03).[1]

The single-crystal X-ray diffraction data of **4a**, **4b** and **5** were collected on a Rigaku

SCX-mini diffractometer at 293(2)K. The program CrystalClear2 was used for the integration of the diffraction profiles. The structure was solved by direct method using the SHELXS program of the SHELXTL package and refined by full-matrix least-squares methods with SHELXL (semi-empirical absorption corrections were applied by using the SADABS program).[3] The non-hydrogen atoms were located in successive difference Fourier syntheses and refined with anisotropic thermal parameters on F2. All hydrogen atoms were generated theoretically onto the specific atoms and refined isotropically with fixed thermal factors.

Calculations were performed using the Gaussian 09 computational programme.[4] Geometrical optimizations were carried out using the B3LYP density functional method[5] and 6-311+G(2d,p) basis set. The default self-consistent reaction field polarizable continuum model[6] was employed to mimic solvation effects. Nucleus independent chemical shifts (NICS) were calculated using the gauge invariant atomic orbital (GIAO) approach at the same level of theory. NICS(1) values were averaged by two positions (above and below the plane) of all the equivalent rings[7].

2. Synthesic procedures

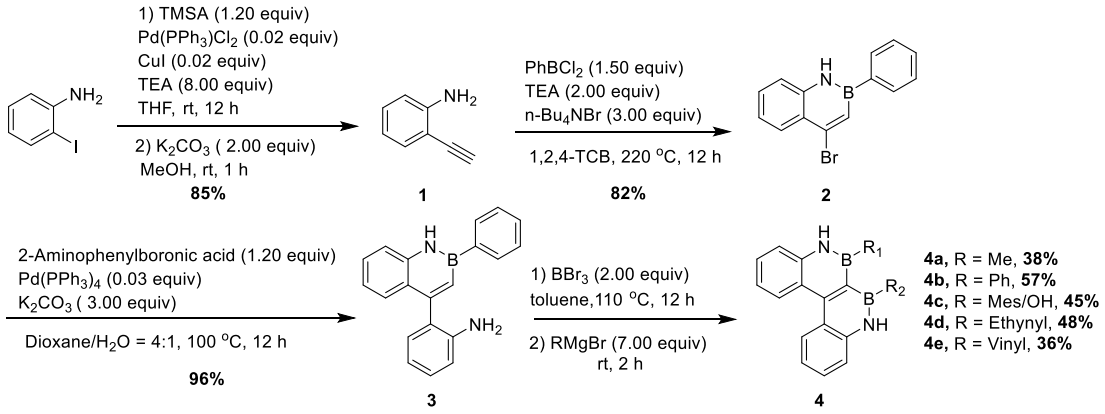

Scheme S1. Synthesis of dual BN-doped [4]helicenes.

Synthesis of 1:

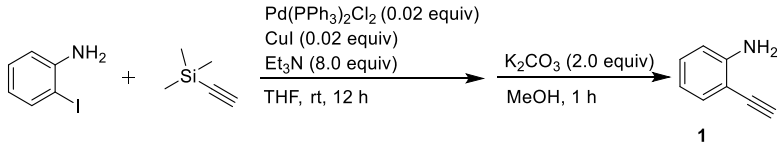

Scheme S2. Synthesis of 1.

A mixture of 2-iodoanilines (8.94 g, 40.82 mmol, 1.0 equiv), $Pd(PPh_3)_2Cl_2$ (576 mg, 0.82 mmol, 0.02 equiv), CuI (156 mg, 0.82 mmol, 0.02 equiv), TMSA (4.81g, 48.98 mmol, 1.20 equiv), and TEA (33.0 g, 326.56 mmol, 8.0 equiv) in THF (50.0 mL) was stirred under nitrogen at room temperature for 12 hours, when the reaction complete, TEA and THF was removed under reduced pressure, and the residues were purified by column chromatography on silica gel (eluent: PE/EA=10:1). The crude product was dissolved in CH_3OH (100.0 mL), K_2CO_3 (11.3 g, 81.64 mmol, 2.0 equiv) was added and the reaction mixture was stirred at room temperature for 1 hour. Then it was concentrated in column and the residue was extracted with EA (15.0 mL × 3) three times, the combined organic layer was washed with brine, dried over anhydrous $MgSO_4$. The solvent was removed under column to give compound **1** as brown oil (4.17 g, yield = 87%, Ref[2]).

^{1}H NMR (400 MHz, $CDCl_3$): δ 7.36 (d, J = 7.2 Hz, 1H, Ar), 7.14-7.18 (m, 1H, Ar), 6.69-6.73 (m, 2H, Ar), 4.27 (br, 2H, NH), 3.42 (s, 1H, CH).

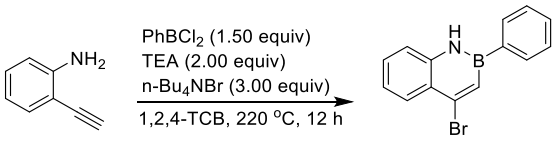

1 2

Scheme S3. Synthesis of **2**.

To a solution of **1** (800 mg, 6.83 mmol, 1.0 equiv) in dry 1,2,4-TCB (80.0 ml) was added TEA (1.38 g, 13.66 mmol, 2.0 equiv), n-Bu_4NBr (6.61 g, 20.49 mmol, 3.0 equiv), and $PhBCl_2$ (1.63 g, 10.24 mmol, 1.5 equiv). Then it was stirred at 220 ºC for 12 h. After cooling to ambient temperature, it was extracted with DCM (15.0 mL × 3) three times. After washed with brine, the combined organic layer was dried over $MgSO_4$, and remove the solvents. The residue was purified by column chromatography on silica gel (eluent: PE/EA = 1/0 ~ 10/1) to give **2** as colorless oil (1.59 g, yield = 82%).

^1H NMR (400 MHz, $CDCl_3$): δ 8.19-8.24 (m, 1H, Ar), 8.09 (br, 1H, NH), 7.87-7.90 (m, 2H, Ar), 7.75 (s, 1H, Ar), 7.50-7.53 (m, 4H, Ar), 7.28-7.35 (m, 2H, Ar). ^{13}C NMR (100 MHz, $CDCl_3$): δ 140.9, 139.6, 132.6, 130.0, 129.8, 129.6, 128.3, 124.2, 122.0, 118.6 ppm (B-aryl carbon was not observed). ^{11}B NMR (128 MHz, $BF_3 \cdot OEt_2$): δ 33.6 ppm. FTIR (thin film): 3385, 2922, 1609, 1555, 1419, 1349, 1267, 1094, 912, 756 cm^{-1}. ESI-HRMS: calcd for $C_{14}H_{11}BBrN$ $[M + H]^+$: 284.0241; Found: 284.0239.

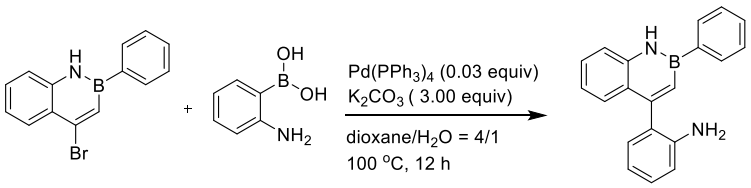

2 3

Scheme S4. Synthesis of **3**.

To a solution of **2** (617 mg, 2.17 mmol, 1.0 equiv) in dioxane/H_2O (20.0 mL/5.0 mL) under nitrogen was added 2-aminophenylboronic acid (357 mg, 2.60 mmol, 1.2 equiv), $Pd(PPh_3)_4$ (81 mg, 0.07 mmol, 0.03 equiv), K_2CO_3 (900 mg, 6.51 mmol, 3.0 equiv). Then it was stirred at 100 ºC for 12 hours. After cooling to ambient temperature, the solvent was removed under reduced pressure, and the residue was extracted with DCM (15.0 mL × 3) three times. After washed with brine, the combined organic layer was dried over $MgSO_4$. Solvent was removed by vacuum, the residue was purified by column chromatography on silica gel (eluent: PE/EA = 10/1) to give **3** as white solid (616 mg, yield = 96%).

M.p. (138-140 ºC); ^{1}H NMR (400 MHz, $CDCl_3$): δ 8.25 (br, 1H, NH), 7.95-7.99 (m, 2H, Ar), 7.46-7.53 (m, 5H, Ar), 7.40-7.43 (m, 1H, Ar), 7.26-7.31 (m, 2H, Ar), 7.20 (dd, J_1 = 7.6 Hz, J_2 = 1.2 Hz, 1H, Ar), 7.14 (t, J = 6.8 Hz, 1H, Ar), 6.93 (t, J = 7.6 Hz, 1H, Ar), 6.86 (d, J = 8.0 Hz, 1H, Ar), 3.54 (br, 2H, NH_2). ^{13}C NMR (100 MHz, $CDCl_3$): δ 154.1, 143.3, 140.7, 137.6 132.7, 130.0, 129.7, 128.7, 128.6, 128.2, 128.03, 127.98, 124.3, 121.3, 118.7, 118.3, 115.4 ppm (B-aryl carbon was not observed). ^{11}B NMR (128 MHz, $BF_3{\cdot}OEt_2$): δ 33.5 ppm. FTIR (thin film): 3379, 2920, 2850, 1611, 1558, 1493, 1409, 1296, 753, 704 cm^{-1}. ESI-HRMS: calcd for $C_{20}H_{17}N_2B$ $[M + H]^+$: 297.1558; Found: 297.1561.

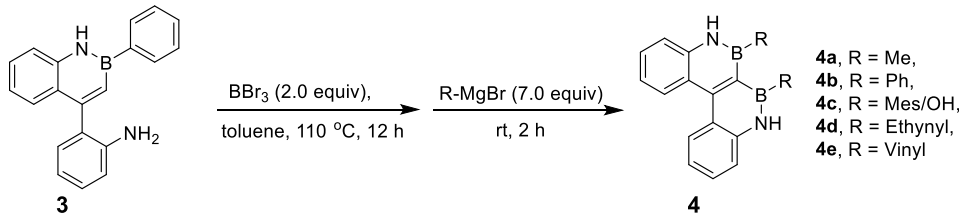

Scheme S5. Synthesis of **4**.

To a solution of **3** (1.0 equiv) in toluene under nitrogen was added BBr_3 (2.0 equiv), then the mixture was stirred at 110 ºC for 12 h. After cooling to ambient temperature, Grignard reagent (7.0 equiv) was added and stirred for another 2 hours. When the reaction completed monitored by TLC plate, the mixture was poured into water and extracted with EA (15.0 mL × 3) three times. After washed with brine, the combined organic layer was dried over $MgSO_4$. Solvents was removed, the residue was purified by column chromatography on silica gel (eluent: PE/EA = 10/1) to give **4**.

4a, yield = 38%, white solid, M.p. (160-163ºC); ^{1}H NMR (400 MHz, $CDCl_3$): δ 8.40 (d, J = 8.0 Hz, 2H, Ar), 7.54 (br, 2H, Ar), 7.46 (t, J = 7.2 Hz, 2H, Ar), 7.27 (d, J = 8.8 Hz, 2H, Ar), 7.17 (dd, J_1 = 8.0 Hz, J_2 = 7.2 Hz, 2H, Ar), 1.02 (s, 6H, CH_3). ^{13}C NMR (100 MHz, $CDCl_3$): δ 154.3, 142.1, 130.5, 128.5, 122.9, 119.5, 118.1 ppm (B-aryl carbons were not observed). ^{11}B NMR (128 MHz, $BF_3{\cdot}OEt_2$): δ 39.7 ppm. FTIR (thin film): 3376, 2919, 2850, 1976, 1648, 1531, 1469, 1368, 1078, 751, 420 cm^{-1}. ESI-HRMS: calcd for $C_{16}H_{16}N_2B_2$ $[M+H]^+$: 259.1572; Found: 259.1572.

4b, yield = 57%, white solid, M.p. (264-266 ºC); ^{1}H NMR (400 MHz, $CDCl_3$): δ 8.49 (d, J = 8.4 Hz, 2H, Ar), 7.86 (br, 2H, Ar), 7.56 (t, J = 8.0 Hz, 2H, Ar), 7.42 (dd, J_1 = 8.4 Hz, J_2 = 1.2 Hz, 2H, Ar), 7.25-7.33 (m, 6H, Ar), 7.07 (t, J = 7.6 Hz, 2H, Ar), 7.00 (t, J

= 7.2 Hz, 4H, Ar). ^{13}C NMR (100 MHz, $CDCl_3$): δ 158.0, 142.0, 133.4, 130.6, 129.2, 127.3, 126.7, 123.4, 120.3, 118.8 ppm (B-aryl carbons were not observed). ^{11}B NMR (128 MHz, $BF_3{\cdot}OEt_2$): δ 37.6 ppm. FTIR (thin film): 3370, 2920, 2850, 1976, 1523, 1424, 1370, 753, 700, 420 cm^{-1}. ESI-HRMS: calcd for $C_{26}H_{20}N_2B_2$ $[M+H]^+$: 383.1885; Found: 383.1885.

4c, yield = 45%, white solid, M.p. (196-200 ºC); ^{1}H NMR (400 MHz, $CDCl_3$): δ 8.57 (d, *J* = 8.4 Hz, 1H, Ar), 8.42 (d, *J* = 8.0 Hz, 1H, Ar), 7.76 (br, 1H, NH), 7.52 (t, *J* = 8.0 Hz, 1H, Ar), 7.43 (t, *J* = 7.6 Hz, 1H, Ar), 7.33 (d, *J* = 8.4 Hz, 1H, Ar), 7.28 (t, *J* = 8.4 Hz, 1H, Ar), 7.10-7.14 (m, 2H, Ar), 7.01 (s, 2H, Ar), 6.75 (br, 1H, NH), 4.33 (s, 1H, BOH), 2.40 (s, 3H, CH_3), 2.21 (s, 6H, CH_3). ^{13}C NMR (100 MHz, $CDCl_3$): δ 157.3, 143.6, 142.2, 140.2, 138.5, 130.5, 130.1, 129.2, 128.8, 128.0, 123.3, 121.7, 120.3, 118.9, 118.5, 118.1, 22.8, 21.2 ppm (B-aryl carbons were not observed). ^{11}B NMR (128 MHz, $BF_3{\cdot}OEt_2$): δ 37.7, 30.3 ppm. FTIR (thin film): 3370, 2920, 2852, 1974, 1538, 1383, 1136, 1071, 756, 512 cm^{-1}. ESI-HRMS: calcd for $C_{23}H_{22}N_2B_2O$ $[M+H]^+$: 365.1991; Found: 365.1991.

4d, yield = 48%, light yellow solid, M.p. (200-204 ºC); ^{1}H NMR (400 MHz, $CDCl_3$): *δ* 8.40 (d, *J* = 8.4 Hz, 2H, Ar), 8.10 (br, 2H, NH), 7.48-7.53 (m, 2H, Ar), 7.31-7.34 (m, 2H, Ar), 7.20-7.25 (m, 2H, Ar), 3.03 (s, 2H, CH). ^{13}C NMR (100 MHz, $CDCl_3$): δ 156.2, 141.7, 130.5, 129.4, 122.8, 120.7, 118.6, 94.3 ppm (B-aryl carbons were not observed). ^{11}B NMR (128 MHz, $BF_3{\cdot}OEt_2$): δ 28.1 ppm. FTIR (thin film): 2957, 2919, 2850, 1976, 1543, 1384, 1133, 1078, 751 cm^{-1}. ESI-HRMS: calcd for $C_{18}H_{12}N_2B_2$ $[M+H]^+$: 279.1259; Found: 279.1259.

4e, yield = 36%, white solid, M.p. (118-120 ºC); ^{1}H NMR (400 MHz, $CDCl_3$): δ 8.41 (d, *J* = 8.4 Hz, 2H, Ar), 7.79 (br, 2H, NH), 7.46-7.51 (m, 2H, Ar), 7.34-7.37 (m, 2H, Ar), 7.17-7.22 (m, 2H, Ar), 7.05-7.14 (m, 2H, Ar), 5.94-5.97 (m, 2H, Ar), 5.91 (s, 2H, Ar). ^{13}C NMR (100 MHz, $CDCl_3$): δ 156.1, 142.1, 141.6 (B-C), 130.5, 128.9, 127.1, 123.3, 120.0, 118.6 ppm (B-aryl carbon was not observed). ^{11}B NMR (128 MHz, $BF_3{\cdot}OEt_2$): δ 34.9 ppm. FTIR (thin film): 2920, 2851, 2377, 2311, 1923, 1526, 1079, 755 cm^{-1}. ESI-HRMS: calcd for $C_{18}H_{16}N_2B_2$ $[M+H]^+$: 283.1572; Found: 283.1571.

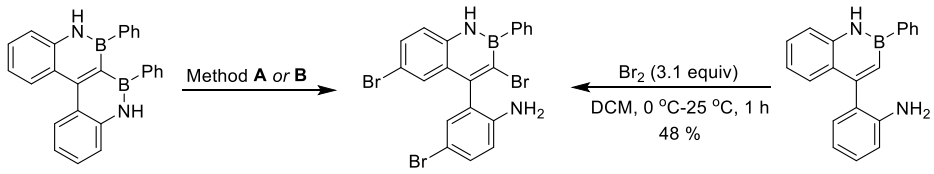

Method **A**: Br_2 (2.2 equiv), DCM, 0 °C-25 °C, 1 h, 44%
Method **B**: NBS (3.0 equiv), $AlCl_3$ (3.0 equiv), DCM, -35 °C, 2 h, 35%

Scheme S6. Investigation of bromination reactions of **5**.

Method A: To a solution of **4b** (1.0 equiv) in DCM under nitrogen was added Br_2 (2.2 equiv) (1.0 M in DCM), the mixture was stirred under 0 °C for 10 min, then it was allowed to room temperature and stirred at the same temperature for 1 hour. When the reaction completed, the mixture was poured into water and extracted with DCM (15.0 mL × 3) three times. After washed with brine, the combined organic layer was dried over $MgSO_4$. Solvents was removed under vacuum, the residue was purified by column chromatography on silica gel (eluent: PE/EA = 4/1) to give **5** as major product (yield = 44%), accompanying with several unidentified byproducts.

It should be noted that **5** can also be synthesized from **3** in 48% yield using similar method.

Method B: A mixture of NBS (3.0 equiv) and $AlCl_3$ (3.0 equiv) in DCM was stirred at room temperature for 30 min under nitrogen. The reaction mixture was cooled down to -35 °C, then **4b** (1.0 equiv) was added at -35 °C. The mixture was stirred at -35 °C for additional 2 hours. When the reaction completed, the mixture was poured into water and extracted with DCM (15.0 mL × 3) three times. After washed with brine, the combined organic layer was dried over MgSO4. Solvents was removed under vacuum, the residue was purified by column chromatography on silica gel (eluent: PE/EA = 4/1) to give **5** as white solid (yield = 35%). white solid, M.p. (188-192 °C), ^{1}H NMR (400 MHz, $CDCl_3$): δ 8.13 (br, 1H, NH), 7.86-7.90 (m, 2H, Ar), 7.57 (dd, J_1 = 8.8 Hz, J_2 = 2.4 Hz, 1H, Ar), 7.47-7.50 (m, 3H, Ar), 7.39-7.42 (m, 2H, Ar), 7.23 (d, J = 8.4 Hz, 1H, Ar), 7.14 (d, J = 2.4 Hz, 1H, Ar), 6.77 (d, J = 8.4 Hz, 1H, Ar), 3.54 (br, 2H, NH_2). ^{13}C NMR (100 MHz, $CDCl_3$): δ 150.5, 142.1, 138.3, 133.3, 132.2, 131.7, 130.3, 130.1, 129.6, 127.9, 127.0, 125.6, 120.1, 117.6, 115.2, 110.3 ppm (B-aryl carbons were not observed). ^{11}B NMR (128 MHz, $BF_3{\cdot}OEt_2$): δ 34.6 ppm. FTIR (thin film): 3369, 2924, 1616, 1541, 1485, 1422, 1262, 1025, 816, 703 cm^{-1}. ESI-HRMS: calcd for $C_{20}H_{14}BBr_3N_2$ $[M + H]^+$: 530.8873; Found: 530.8874.

Table S1. Condition screening for the synthesis of **4b**.

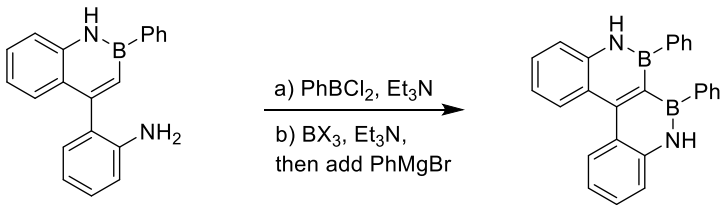

3 **4b**

entry	Boron reagent /equiv	Et_3N / equiv	Solvent	Tem / °C	T / h	Yield
1[a]	$PhBCl_2$ 1.5	2.0	o-DCB	180	12-16	trace
2[a]	$PhBCl_2$ 1.5	3.0	TCB	220	12-16	trace
3[a]	$PhBCl_2$ 2.0	4.0	TCB	220	12-16	16%
4[b]	BCl_3 1.5	2.0	TCB	220	12-16	No
5[b]	BCl_3 1.5	3.0	TCB	220	12-16	trace
6[b]	$BCl_3$2.0	0	TCB	220	12	>19%
7[b]	BBr_3 2.0	0	TCB	220	12	22%
8[b]	BBr_3 2.0	0	TCB	200	12	24%
9[b]	BBr_3 2.0	0	o-DCB	180	12	28%
10[b]	BBr_3 2.0	0	PhCl	135	12	41%
11[b]	BBr_3 2.0	0	PhCl	130	12	32%
12[b]	**BBr_3 2.0**	**0**	**toluene**	**110**	**12**	**55%**
13[b]	BBr_3 2.0	0	toluene	80	12	31%
14[b]	BBr_3 2.0	0.5	toluene	110	12	50%
15[b]	BBr_3 2.0	1.0	toluene	110	12	56%
16[b]	BBr_3 2.0	1.5	toluene	110	12	53%
17[b]	BBr_3 2.0	2.0	toluene	110	12	50%
18[b]	BBr_3 2.0	2.5	toluene	110	12	<10%

3. Computational Details

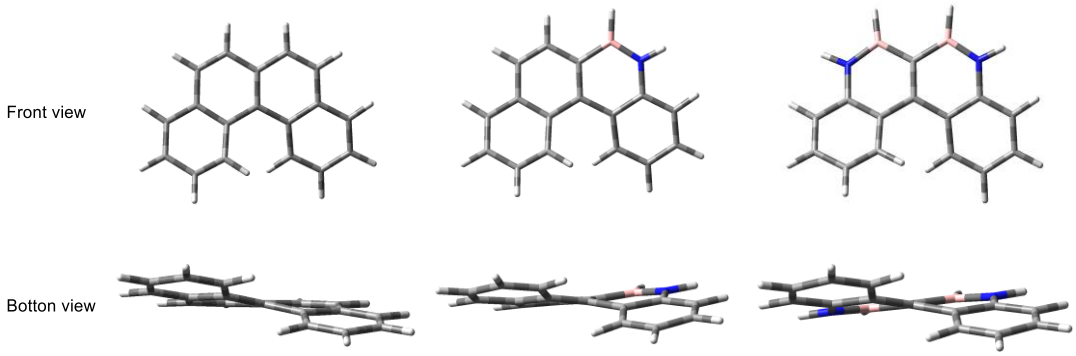

Fig. S1 Optimized structures of **[4]helicene**, **mono-[4]BN-Helicene** and **bis-BN [4]helicene**.

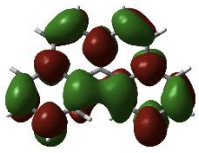	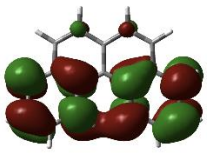	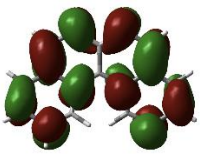	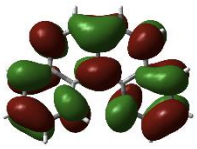
LUMO+3	LUMO+2	LUMO+1	LUMO
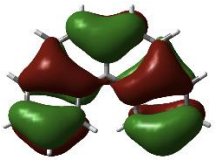	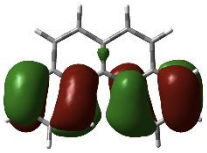	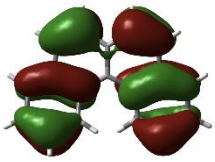	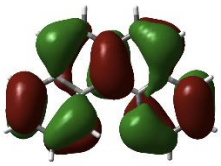
HOMO-3	HOMO-2	HOMO-1	HOMO

Fig. S2 Molecular orbitals contributing to the DFT calculated transitions of **[4]helicene** (iso = 0.02, B3LYP-D3/6-311G(2d,p)).

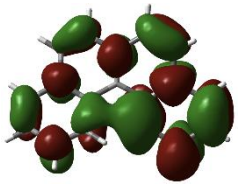	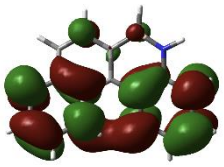	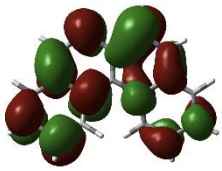	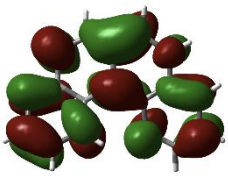
LUMO+3	LUMO+2	LUMO+1	LUMO
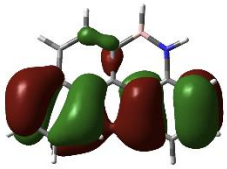	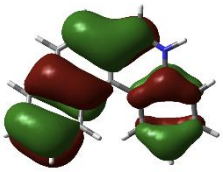	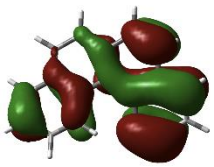	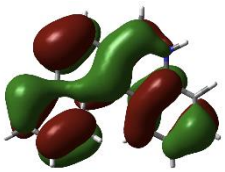
HOMO-3	HOMO-2	HOMO-1	HOMO

Fig. S3 Molecular orbitals contributing to the DFT calculated transitions of **mono-[4]BN-Helicene** (iso = 0.02, B3LYP-D3/6-311G(2d,p)).

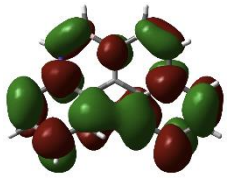	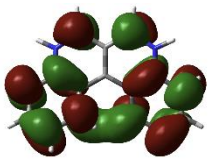	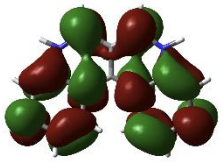	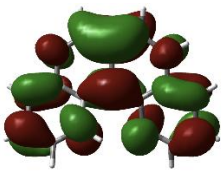
LUMO+3	LUMO+2	LUMO+1	LUMO
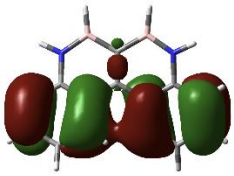	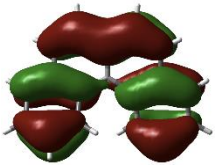	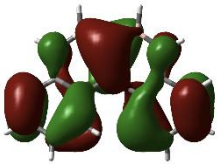	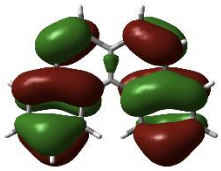
HOMO-3	HOMO-2	HOMO-1	HOMO

Fig. S4 Molecular orbitals contributing to the DFT calculated transitions of **bis-BN [4]helicene** (iso = 0.02, B3LYP-D3/6-311G(2d,p)).

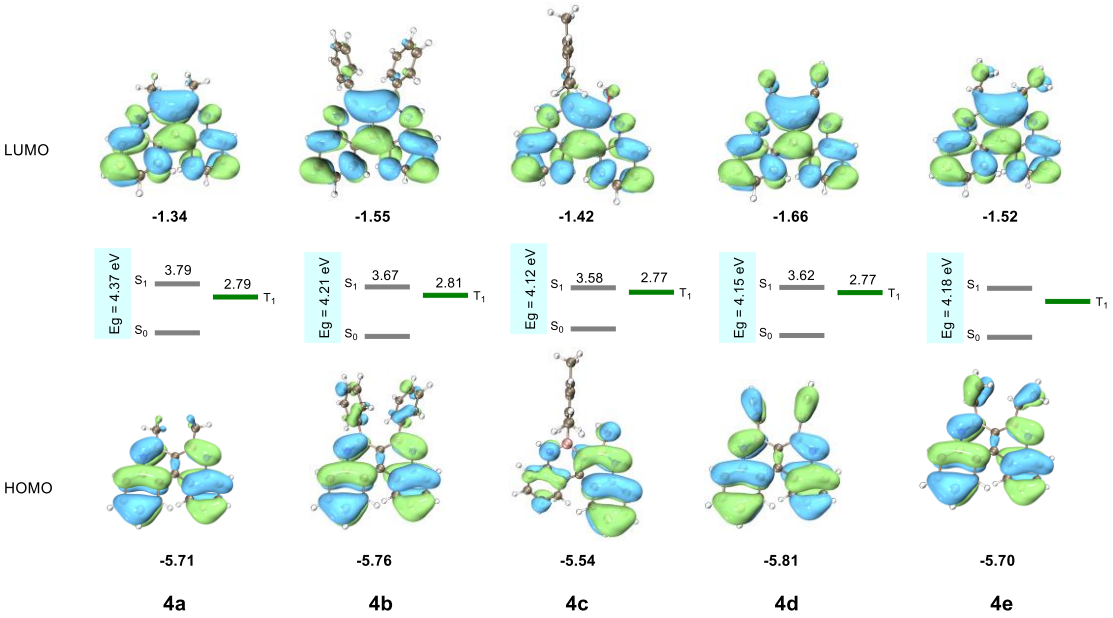

Fig. S5 HOMO and LUMO distributions, energy level diagrams, and oscillator strengths of **4a**-**4e**.

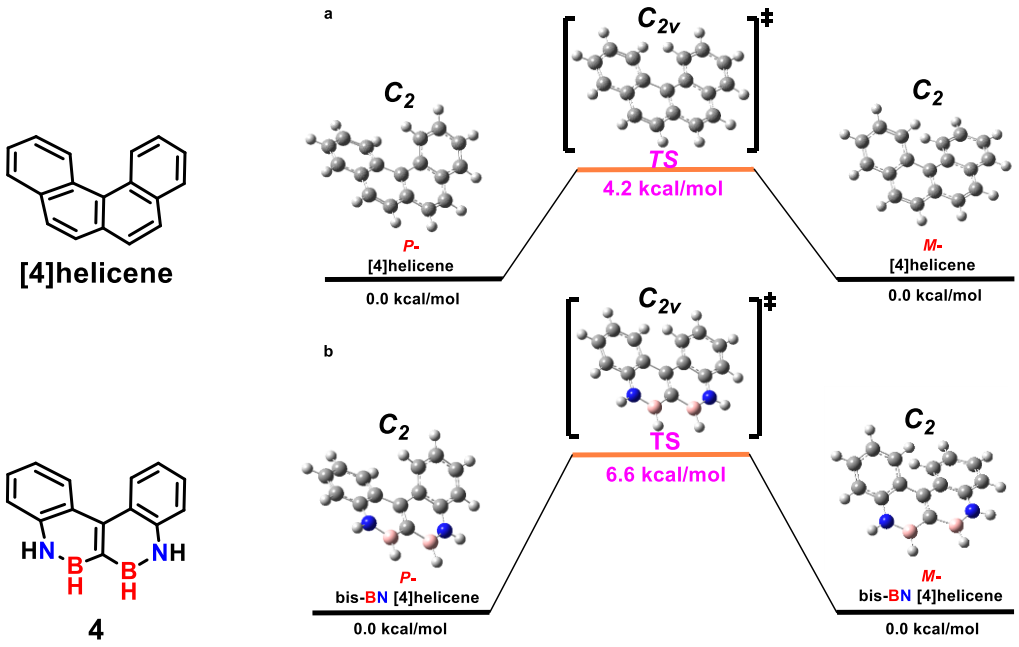

Fig. S6 Isomerization process and relative internal energy (kcal/mol) for **[4]helicene** and **bis-BN [4]helicene**.

4. Single-Crystal X-ray Analysis

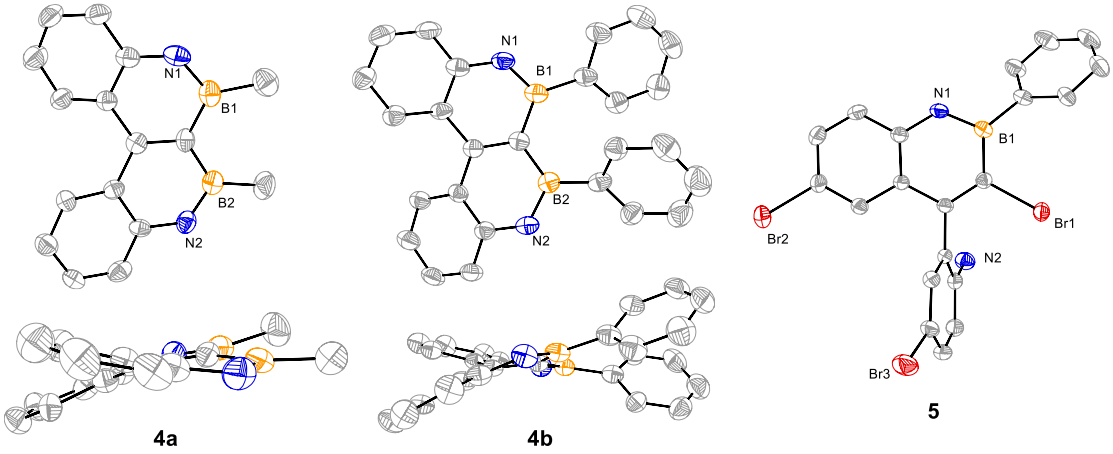

Fig. S7 Single crystal X-ray structures of **4a**, **4b** and **5**, (C: grey, B: orange, N: blue, Br: red. 50% thermal ellipsoids).

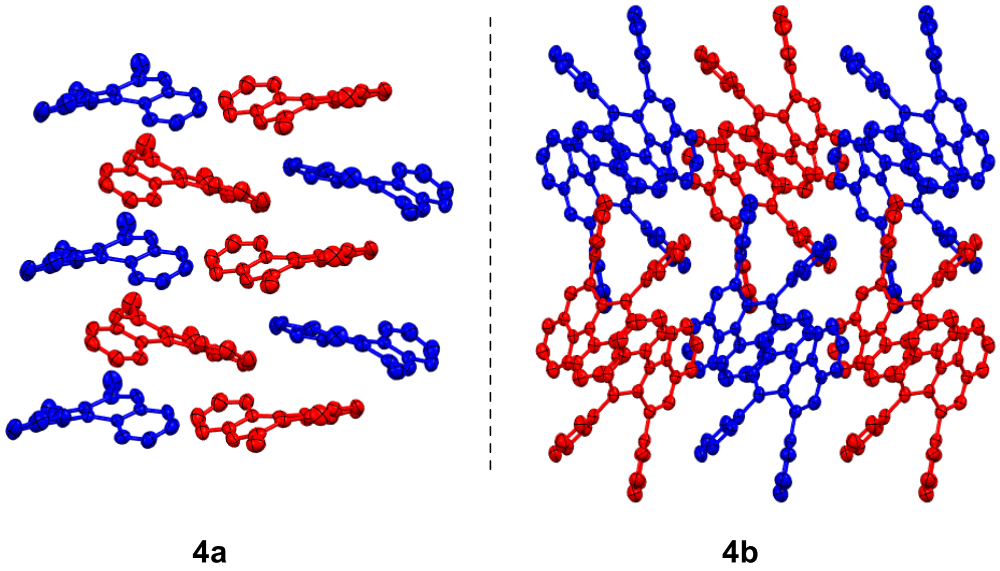

Fig. S8 Packing structure of **4a** and **4b**.

Table S2 Crystal date and structure refinement for **4a** (CCDC: 2524792).

Identification code	**4a**
Empirical formula	$C_{16}H_{16}B_2N_2$
Formula weight	257.93
Temperature/K	293(2)
Crystal system	monoclinic
Space group	Cc
a/Å	19.257(3)
b/Å	18.442(3)
c/Å	7.9702(19)
α/°	90
β/°	99.63(2)
γ/°	90
Volume/Å^3	2790.6(9)
Z	8
ρ_{calc}g/cm^3	1.228
μ/mm^{-1}	0.071
F(000)	1088.0
Crystal size/mm^3	0.22 × 0.2 × 0.18
Radiation	Mo Kα (λ = 0.71073)
2Θ range for data collection/°	5.714 to 50
Index ranges	$-22 \leq h \leq 14$, $0 \leq k \leq 21$, $-9 \leq l \leq 9$
Reflections collected	2934
Independent reflections	2934 [R_{int} = ?, R_{sigma} = 0.0969]
Data/restraints/parameters	2934/2/366
Goodness-of-fit on F^2	0.998
Final R indexes [I>=2σ (I)]	R_1 = 0.0795, wR_2 = 0.1976
Final R indexes [all data]	R_1 = 0.1309, wR_2 = 0.2446
Largest diff. peak/hole / e Å^{-3}	0.24/-0.30
Flack parameter	1.8(10)

Table S3 Crystal date and structure refinement for **4b** (CCDC: 2524793).

Identification code	**4b**
Empirical formula	$C_{26}H_{20}B_2N_2$
Formula weight	382.06
Temperature/K	293(2)
Crystal system	orthorhombic
Space group	Pbca
a/Å	13.4755(11)
b/Å	15.3837(14)
c/Å	19.915(2)
α/°	90
β/°	90
γ/°	90
Volume/Å^3	4128.5(7)
Z	8
ρ_{calc}g/cm^3	1.229
μ/mm^{-1}	0.071
F(000)	1600.0
Crystal size/mm^3	0.22 × 0.2 × 0.18
Radiation	Mo Kα (λ = 0.71073)
2Θ range for data collection/°	5.296 to 49.426
Index ranges	$-6 \leq h \leq 15$, $-18 \leq k \leq 18$, $-19 \leq l \leq 22$
Reflections collected	10524
Independent reflections	3443 [R_{int} = 0.0597, R_{sigma} = 0.0715]
Data/restraints/parameters	3443/0/272
Goodness-of-fit on F^2	1.066
Final R indexes [I>=2σ (I)]	R_1 = 0.0683, wR_2 = 0.1730
Final R indexes [all data]	R_1 = 0.1199, wR_2 = 0.2334
Largest diff. peak/hole / e Å^{-3}	0.23/-0.28

Table S4 Crystal date and structure refinement for **5** (CCDC: 2524794).

Identification code	**5**
Empirical formula	$C_{20}H_{14}BBr_3N_2$
Formula weight	532.87
Temperature/K	293(2)
Crystal system	monoclinic
Space group	I2/a
a/Å	10.5230(8)
b/Å	13.4295(11)
c/Å	26.9791(17)
α/°	90
β/°	91.280(6)
γ/°	90
Volume/Å^3	3811.7(5)
Z	8
ρ_{calc}g/cm^3	1.857
μ/mm^{-1}	6.356
F(000)	2064.0
Crystal size/mm^3	0.12 × 0.1 × 0.08
Radiation	Mo Kα (λ = 0.71073)
2Θ range for data collection/°	6.068 to 56.996
Index ranges	$-14 \leq h \leq 14$, $-17 \leq k \leq 10$, $-36 \leq l \leq 21$
Reflections collected	8735
Independent reflections	4787 [R_{int} = 0.0240, R_{sigma} = 0.0418]
Data/restraints/parameters	4787/0/243
Goodness-of-fit on F^2	1.016
Final R indexes [I>=2σ (I)]	R_1 = 0.0406, wR_2 = 0.0874
Final R indexes [all data]	R_1 = 0.0713, wR_2 = 0.1006
Largest diff. peak/hole / e Å^{-3}	0.99/-0.54

5. Photophysical and Electrochemical Properties

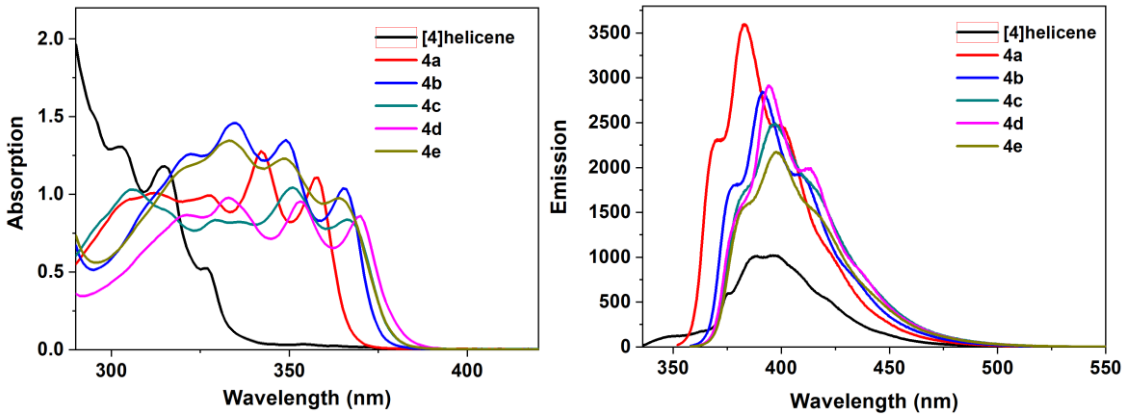

Fig. S9 Unnormalized absorption (left) and emission spectra (right) of carbonaceous **[4]helicene** and **4a-4e** in diluted *n*-hexane solution at a concentration of 10^{-5}

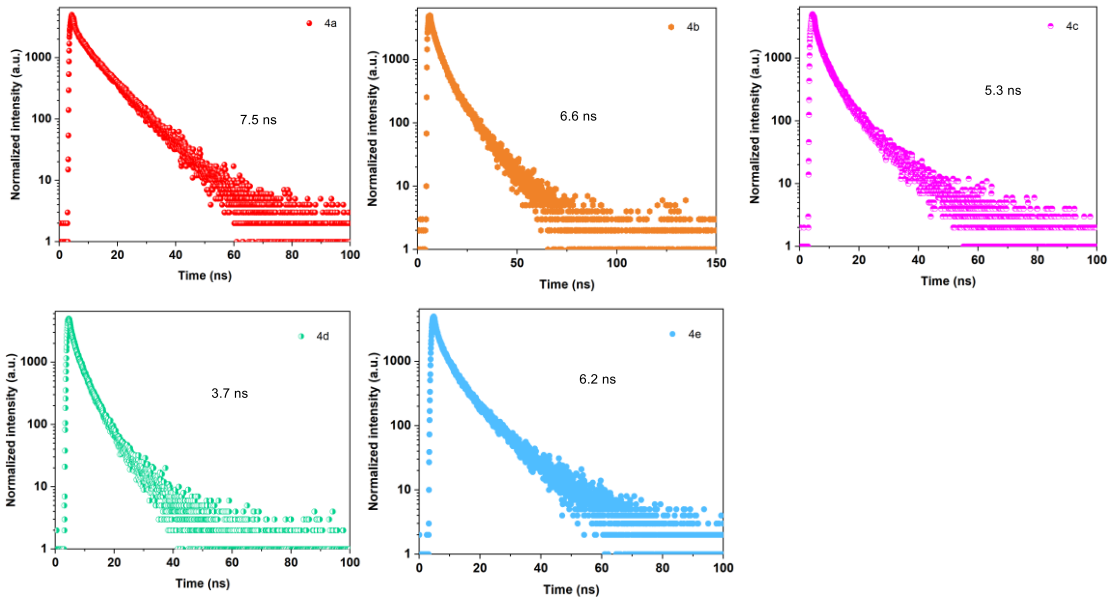

Fig. S10 Transient decay curves of **4a-4e** in toluene solution.

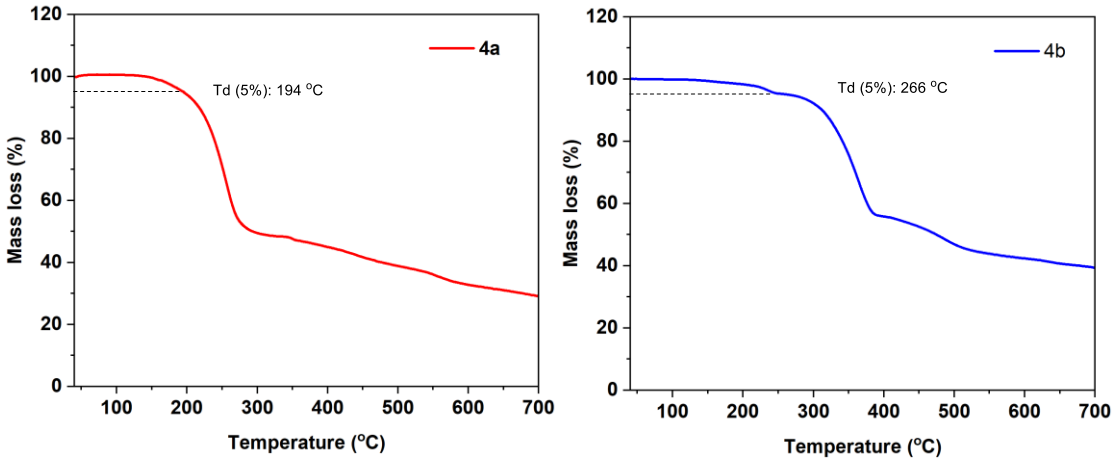

Fig. S11 Decomposition temperature (Td) with 5% weight loss for **4a** and **4b** at a heating rate of 10 °C min^{-1}.

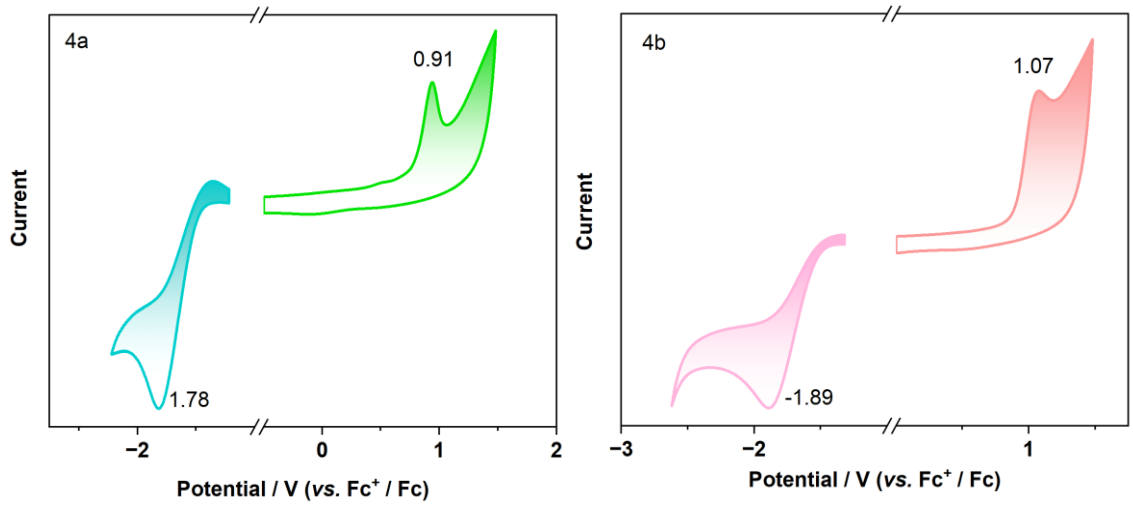

Fig. S12 Cyclic voltammetry curves of **4a** and **4b** showing the oxidation waves in CH_2Cl_2 vs Fc/Fc^+ ($c = 5 \times 10^{-2}$ M), using *n*-Bu_4NPF_6 (0.1 M) as the electrolyte, $v = 100$ mV/s.

Table S5 Summary of photophysical properties of all-carbon [4]helicene and bis-BN helicenes **4a**-**4e**.

Compound	λ_{abs} (nm)	ε 10^4 (M^{-1} cm^{-1})	λ_{onset} (nm)	λ_{ex} (nm)	λ_{em} (nm)	Φ_F[a]	Stokes shift 10^3 (cm^{-1})[b]	E_G^{opt} (eV)[c]	*t* [ns]	k*r* [10^8 s^{-1}][e]	k*nr* [10^8 s^{-1}][f]
[4]helicene	302, 314, 326	1.3, 1.2, 0.5	343	326	345, 375, 388, 395	0.10	1.69	3.62	15.38[d]	0.065	0.59
4a	311, 327, 342, 357	1.0, 1.3, 1.3, 1.1	373	342	369, 382, 400	0.89	0.91	3.32	7.5	1.18	0.15
4b	334, 348, 365	1.5, 1.3, 1.0	380	348	378, 392, 410	0.71	0.94	1.08	6.6	3.26	0.44
4c	305, 350, 366	1.0, 1.0, 0.8	384	350	382, 397, 416	0.79	1.14	3.23	5.3	1.49	0.40
4d	332, 353, 369	1.0, 1.0, 0.9	389	353	381, 394, 413	0.71	0.85	3.19	3.7	1.92	0.78
4e	333, 348, 363	1.3, 1.2, 1.0	385	348	383, 397, 416	0.54	1.44	3.22	6.2	0.87	0.74

[a] Using 9,10-diphenylanthracene as the reference(Φ_F = 0.93); [b] Stokes shift = $1/\lambda_{abs}$ - $1/\lambda_{em}$; [c] Optical band gap E_G^{opt} = $1240/\lambda_{onset}$;
[d] Adopted from reference 8; [e] k$r = F_{PL}/t_F$; [f] knr = 1-F_{PL}/t_F

6. Device Performance

We fabricated two non-doped OLEDs with a configuration of ITO/PEDOT:PSS(40 nm)/emissive layer (EML, 35 nm)/TPBi(30 nm)/LiF(1 nm)/Al(120 nm). The pre-patterned ITO glass substrates were sequentially cleaned by detergent, deionized water, acetone, and isopropanol under the ultrasonic for 20 min. After that, PEDOT: PSS solution was spin-coated on cleaned ITO substrate at 4000 rpm for 30s and annealed to form hole transport layer. Then, the substrates were transferred into the glove box, and the EML, TPBi electron transport layer and LiF/Al composite electrode were successively deposited by a BOC Edwards Auto-500 thermal evaporation system under a pressure of 2×10^{-5} Pa. The film thickness was monitored using in-situ quartz crystal during vacuum deposition. The active area of the device is 0.1 cm^2. The current density-voltage-luminance characteristics and the EL spectra were simultaneously measured with a Photo Research PR-655 spectrophotometer and a Keithley 2450 source meter. The external quantum efficiency (EQE) of the devices was measured using an integrating sphere (Ocean Optics FOIS-1) coupled to a spectrophotometer (QE65Pro).

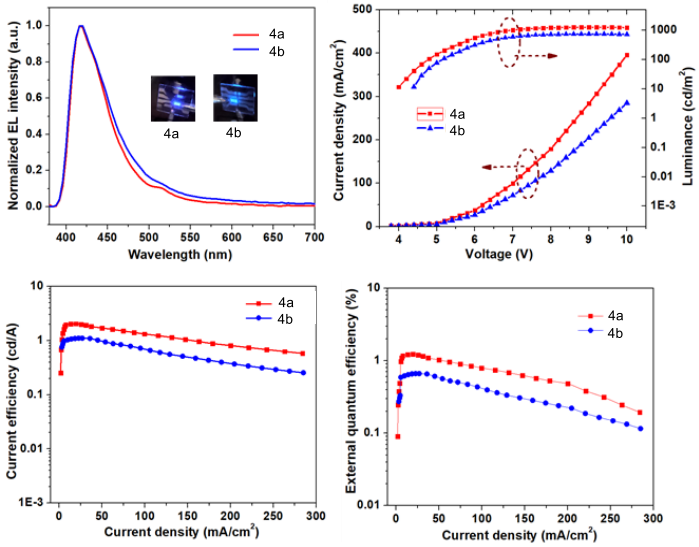

Fig. S13 Fabrication and characterization of OLEDs using **4a** and **4b** as fluorescent dopants (EL spectra, V-I-L characteristics, and power/luminance versus current)

Table S6 Electroluminescence performances of devices base on **4a** and **4b**.

Device	V_{on}	L_{max}	η^{max}	η^{max}	λ_{max}	η_{xt}^{max}	CIE
	V	cd/m^2	cd/A	lm/W	(nm)		(x, y)
4a	3.70	1275	2.00	1.00	416	1.23	(0.17, 0.12)
4b	4.30	752	1.10	0.62	420	0.66	(0.17, 0.15)

V_{on}: Voltage required to reach 1cd cm^{-2}.

7. Characterization by NMR Spectroscopy

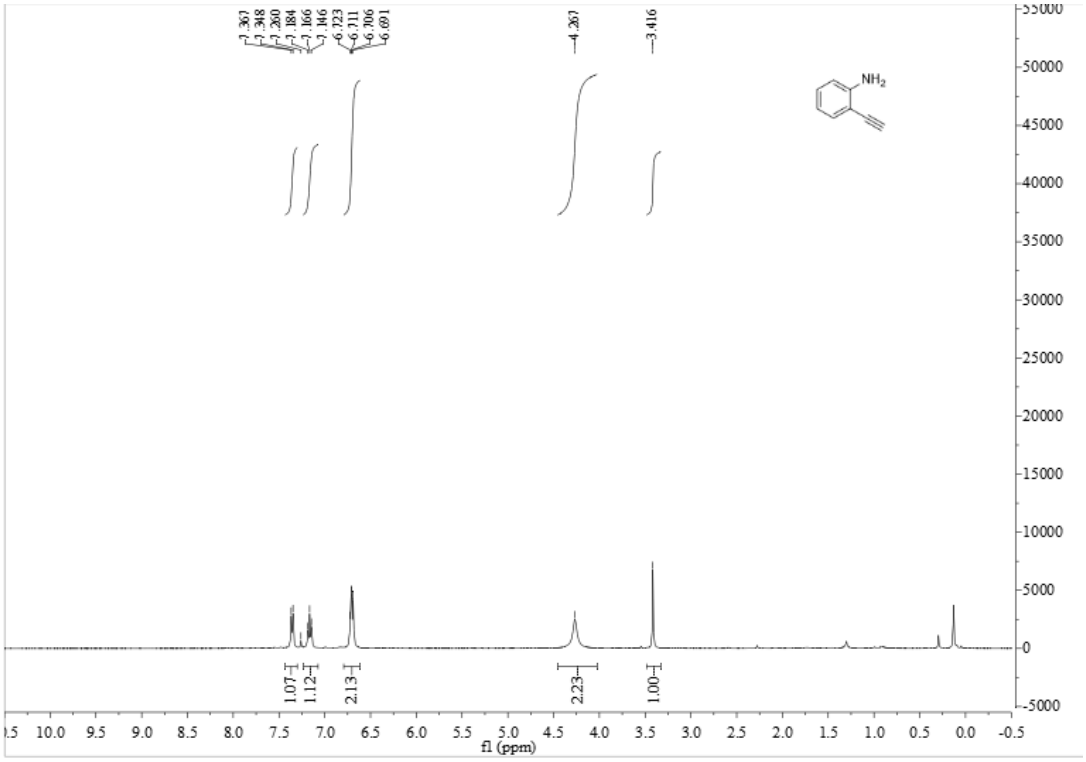

^{1}H NMR spectra of **1** (400 MHz, $CDCl_3$)

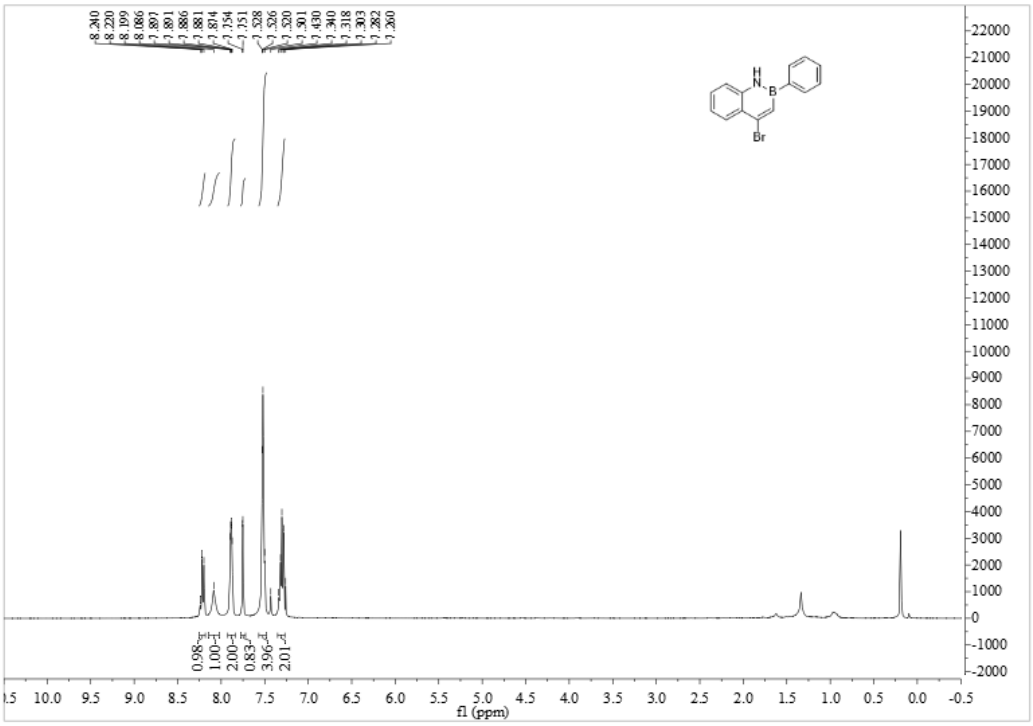

^{1}H NMR spectra of **2** (400 MHz, $CDCl_3$)

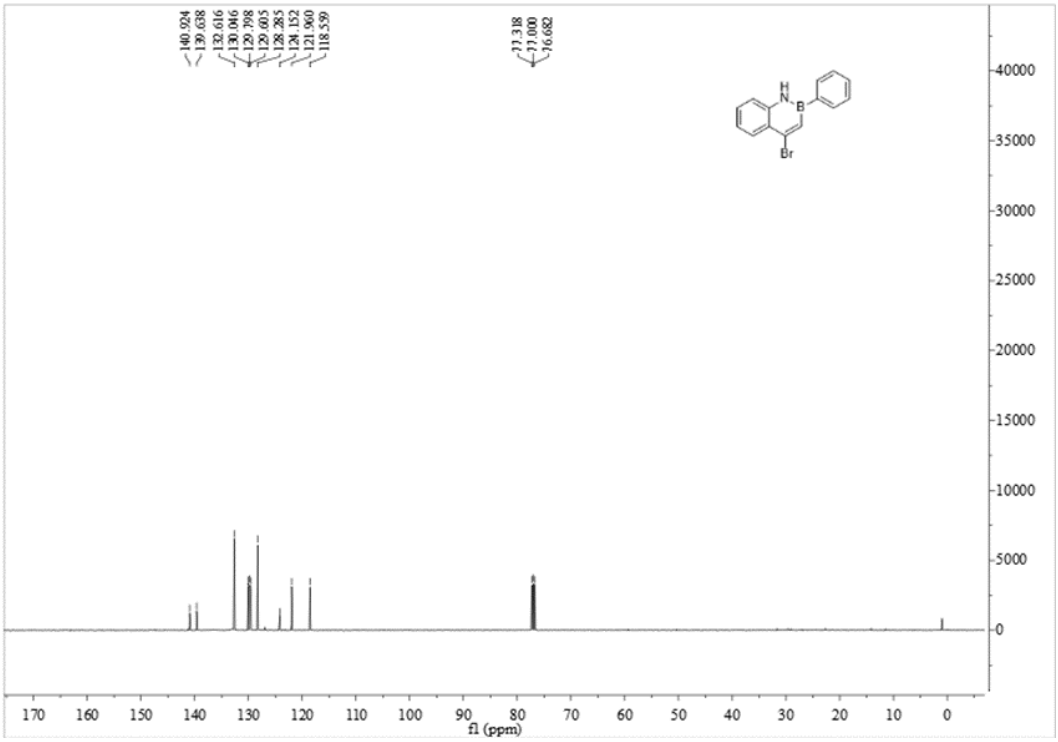

^{13}C NMR spectra of **2** (100 MHz, $CDCl_3$)

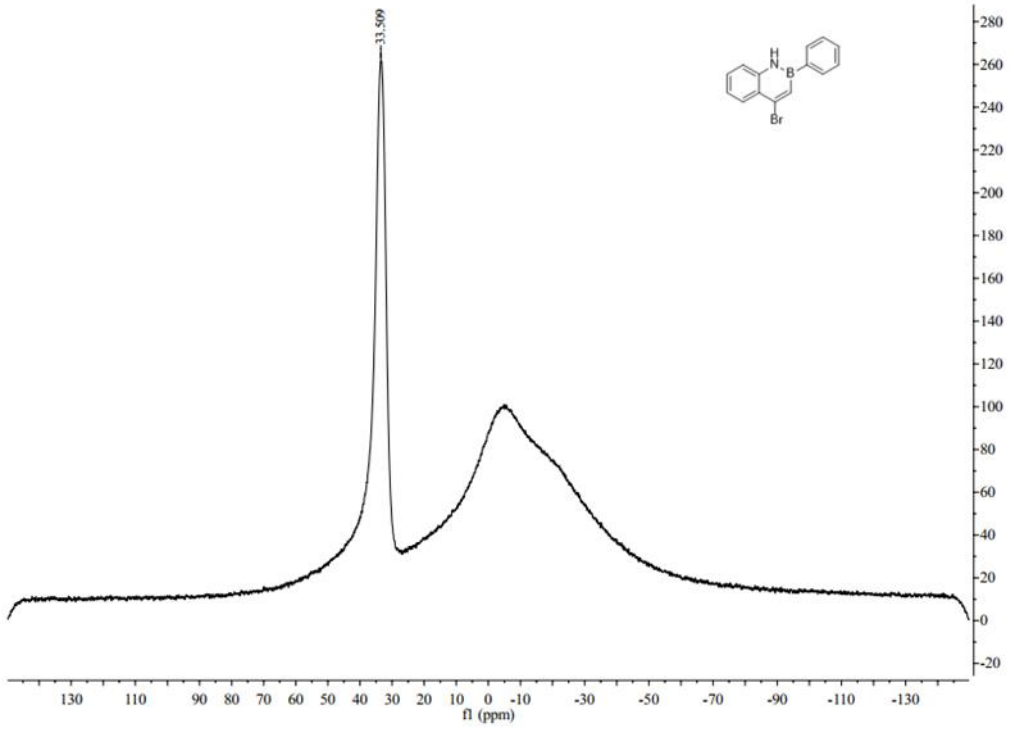

^{11}B NMR spectra of **2** (128 MHz, $CDCl_3$). ^{11}B NMR chemical shifts are reported in ppm relative to external $BF_3{\cdot}OEt_2$ (0 ppm).

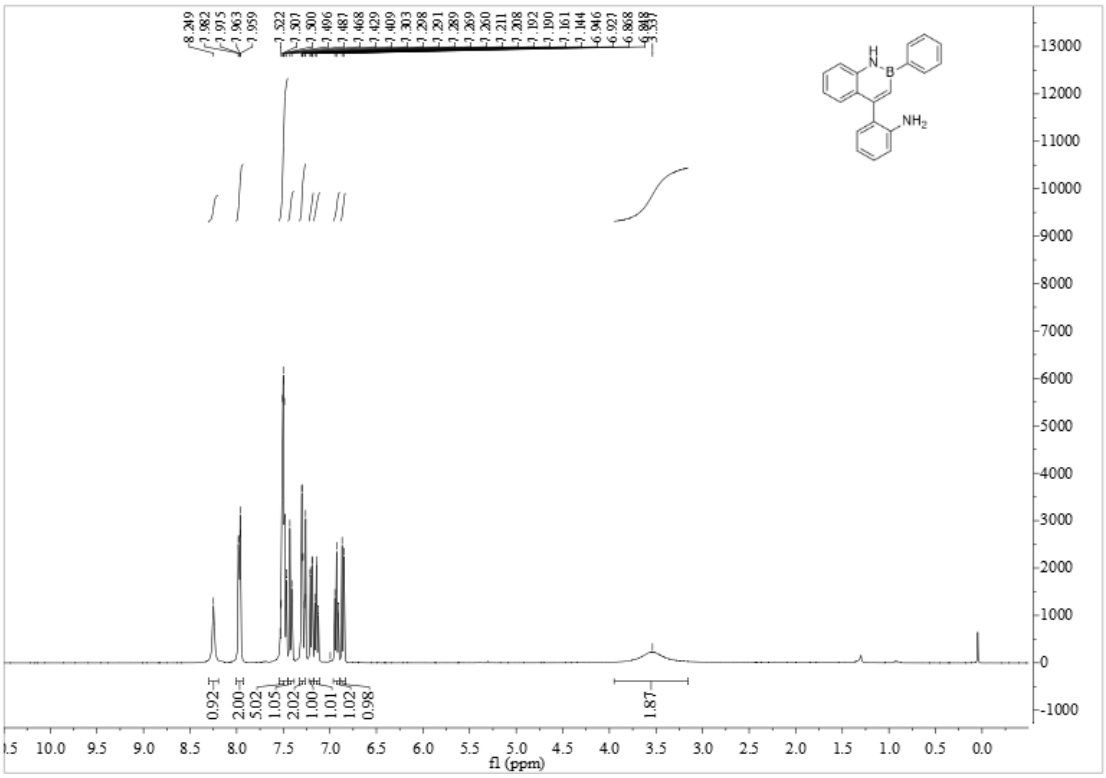

^{1}H NMR spectra of **3** (400 MHz, $CDCl_3$)

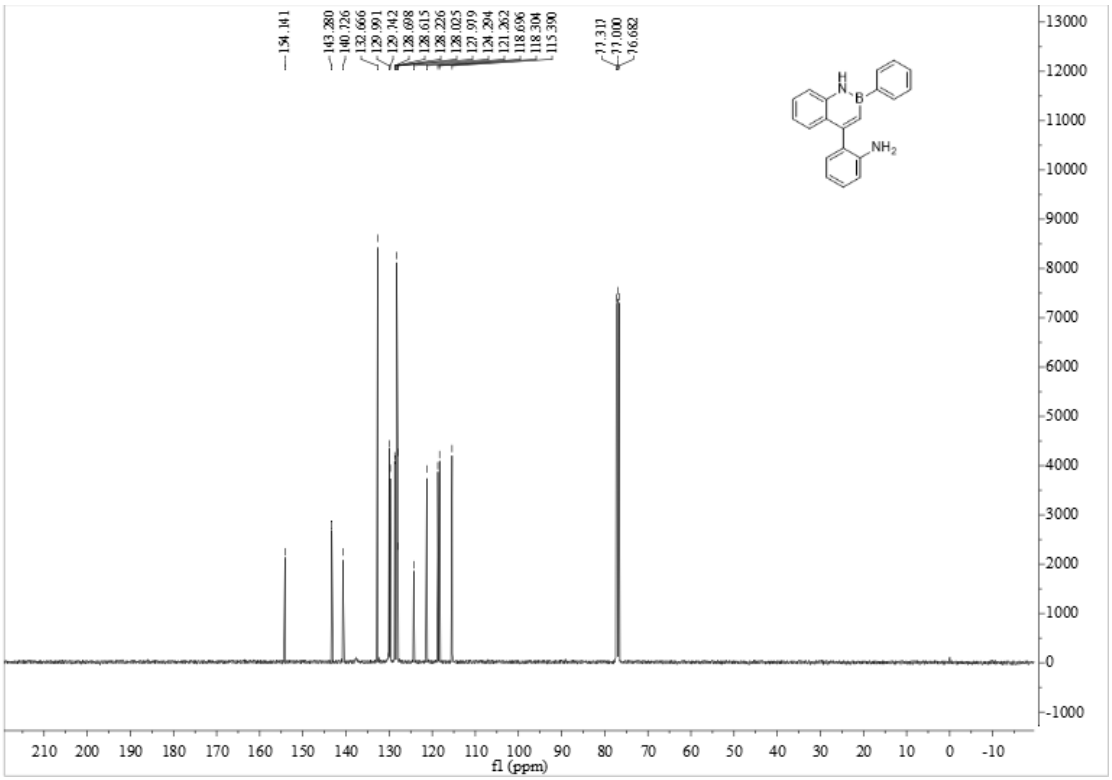

^{13}C NMR spectra of **3** (100 MHz, $CDCl_3$)

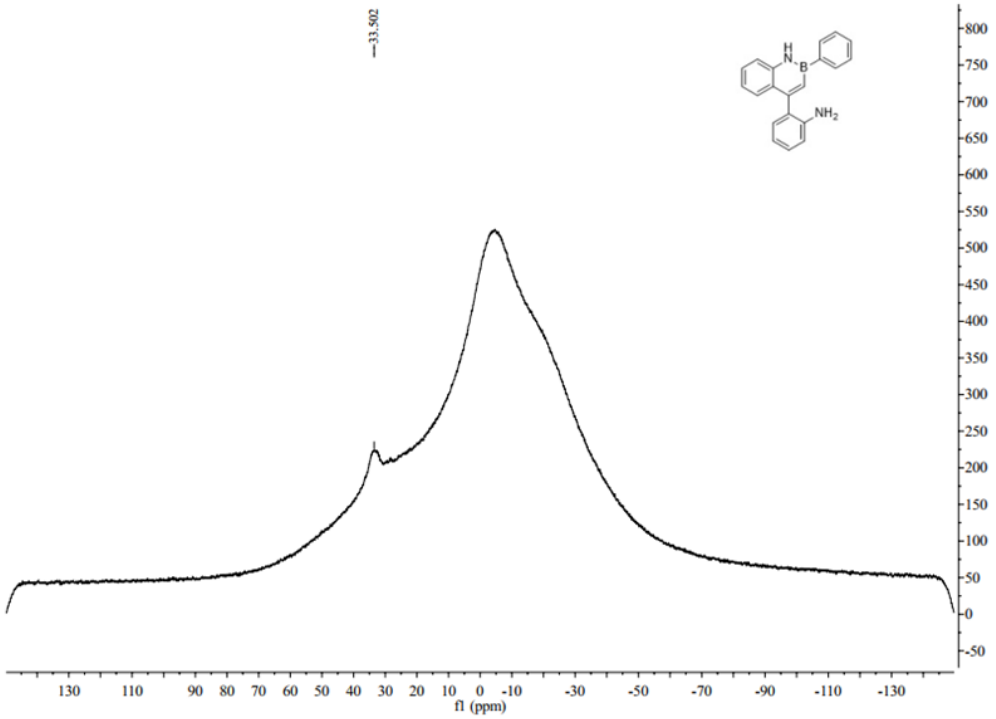

^{11}B NMR spectra of **3** (128 MHz, $CDCl_3$). ^{11}B NMR chemical shifts are reported in ppm relative to external $BF_3{\cdot}OEt_2$ (0 ppm).

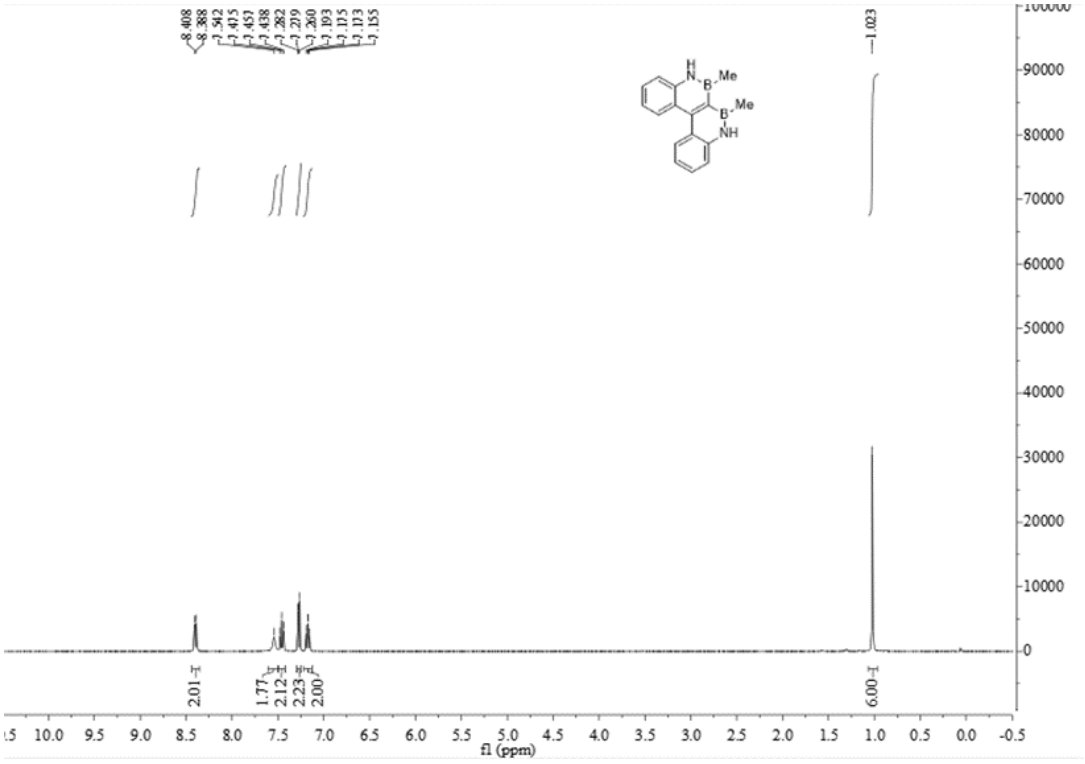

^{1}H NMR spectra of **4a** (400 MHz, $CDCl_3$)

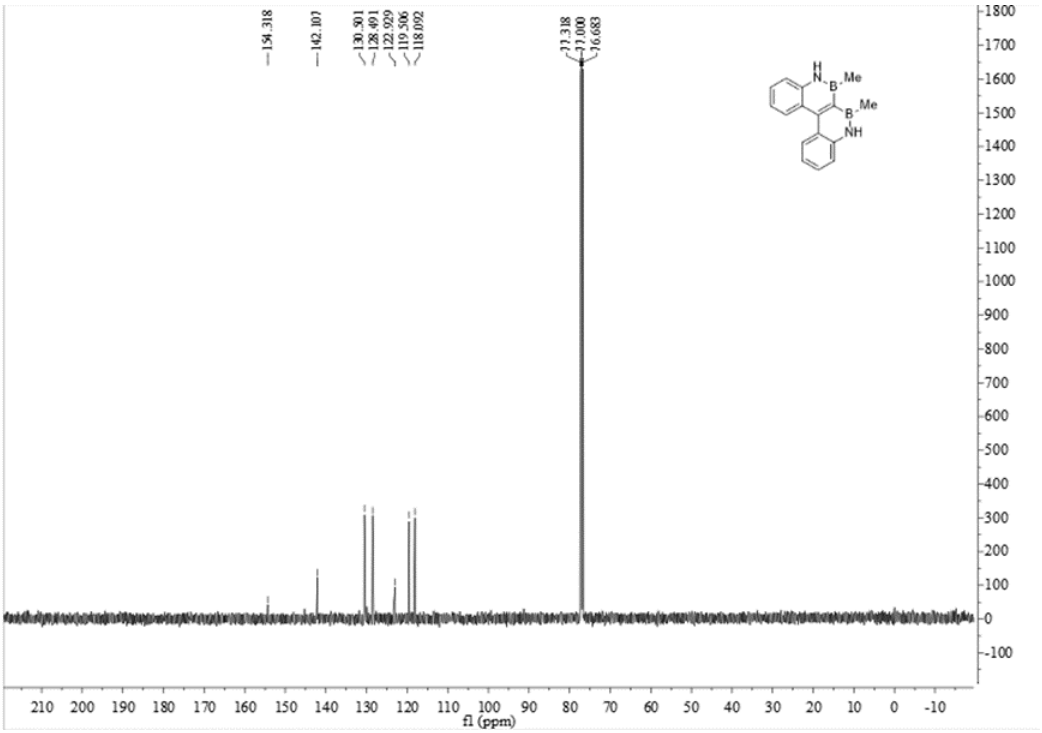

^{13}C NMR spectra of **4a** (100 MHz, $CDCl_3$)

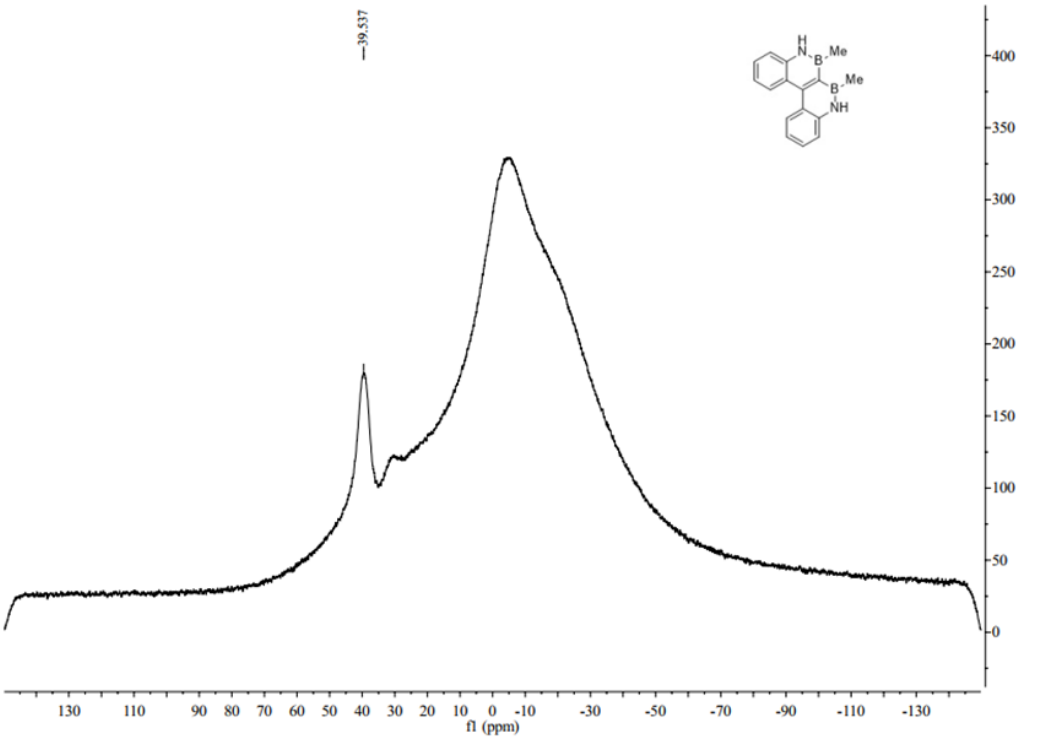

^{11}B NMR spectra of **4a** (128 MHz, $CDCl_3$). ^{11}B NMR chemical shifts are reported in ppm relative to external $BF_3{\cdot}OEt_2$ (0 ppm).

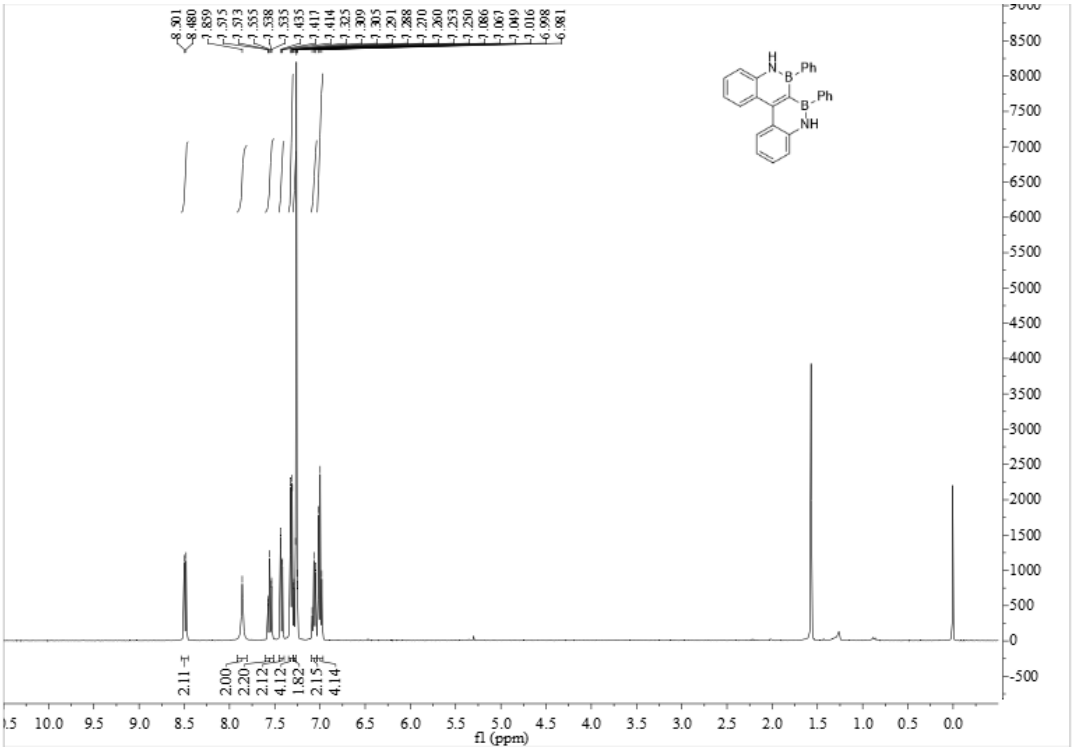

^{1}H NMR spectra of **4b** (400 MHz, $CDCl_3$)

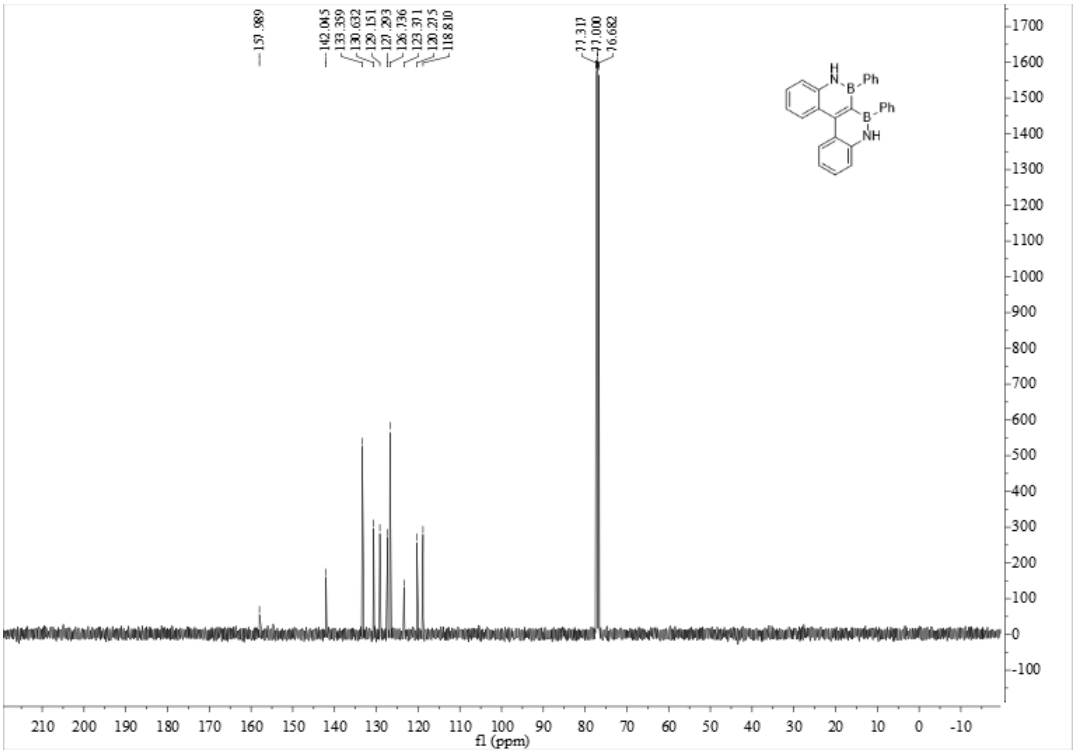

^{13}C NMR spectra of **4b** (100 MHz, $CDCl_3$)

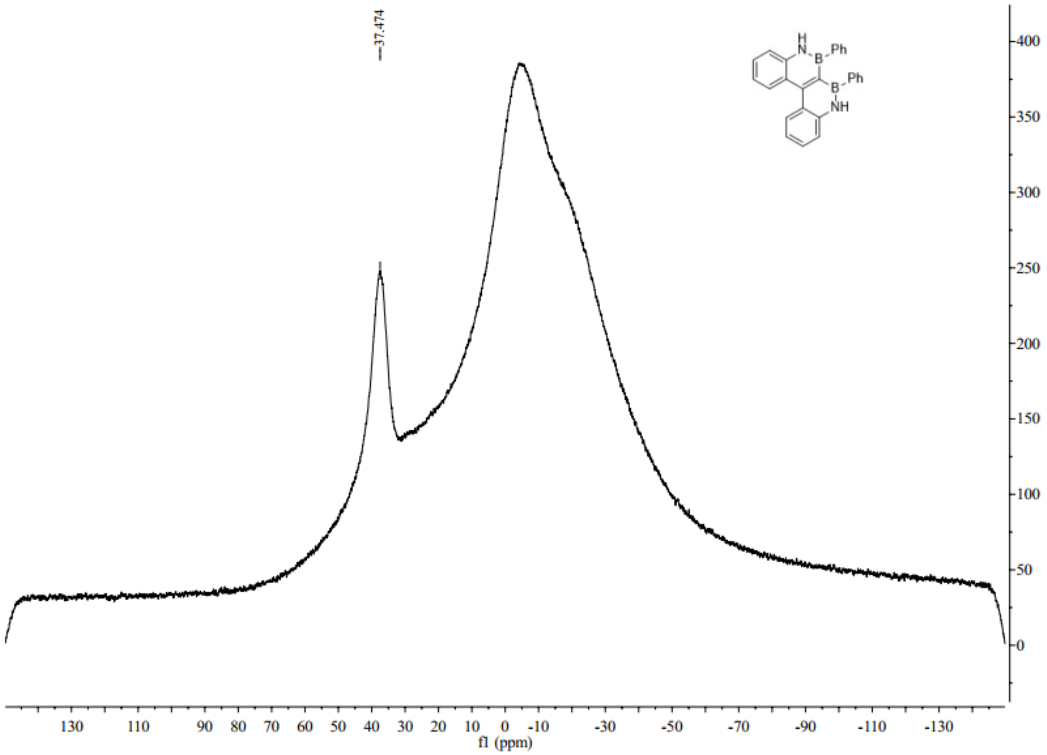

^{11}B NMR spectra of **4b** (128 MHz, $CDCl_3$). ^{11}B NMR chemical shifts are reported in ppm relative to external $BF_3{\cdot}OEt_2$ (0 ppm).

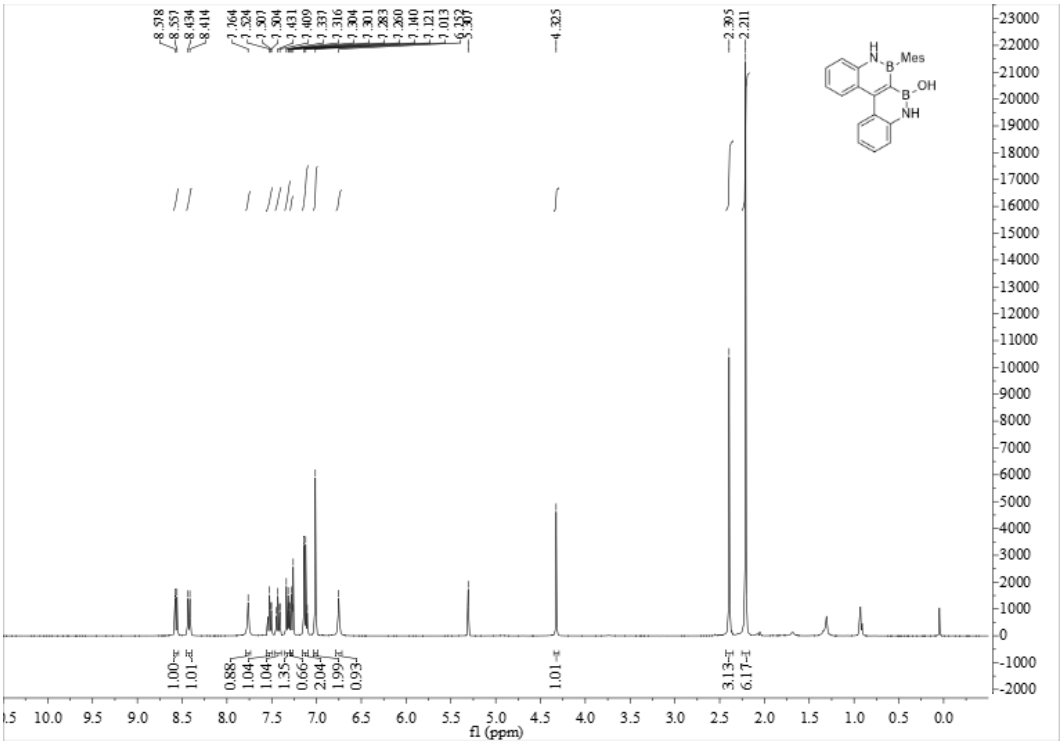

^{1}H NMR spectra of **4c** (400 MHz, $CDCl_3$)

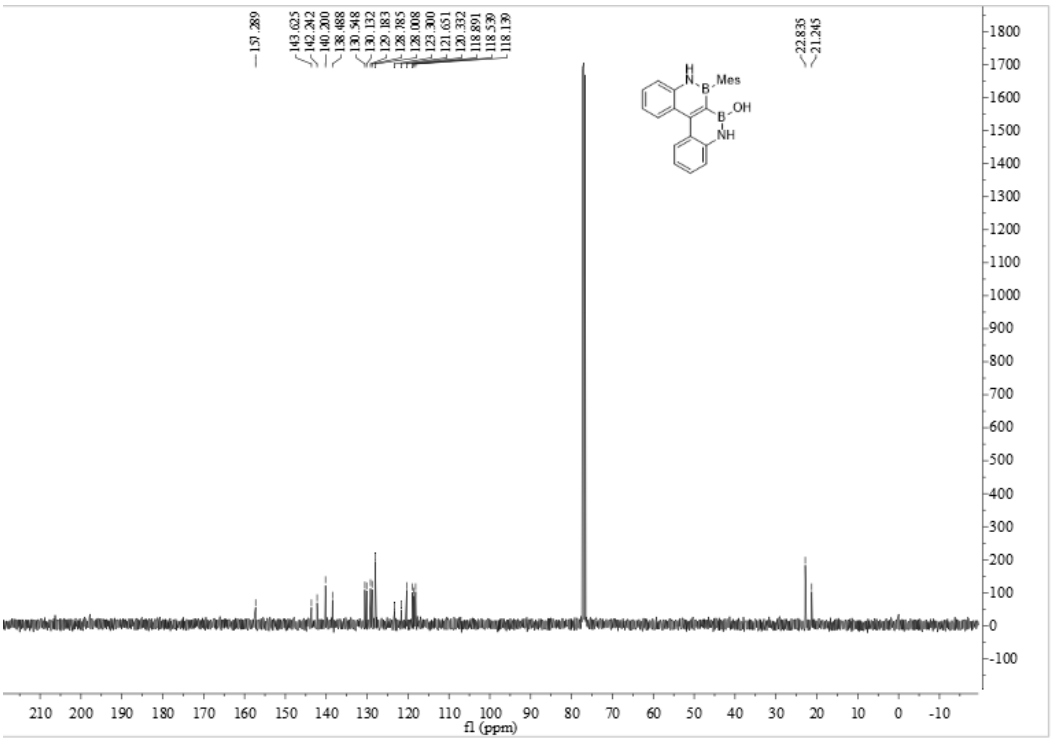

^{13}C NMR spectra of **4c** (100 MHz, $CDCl_3$)

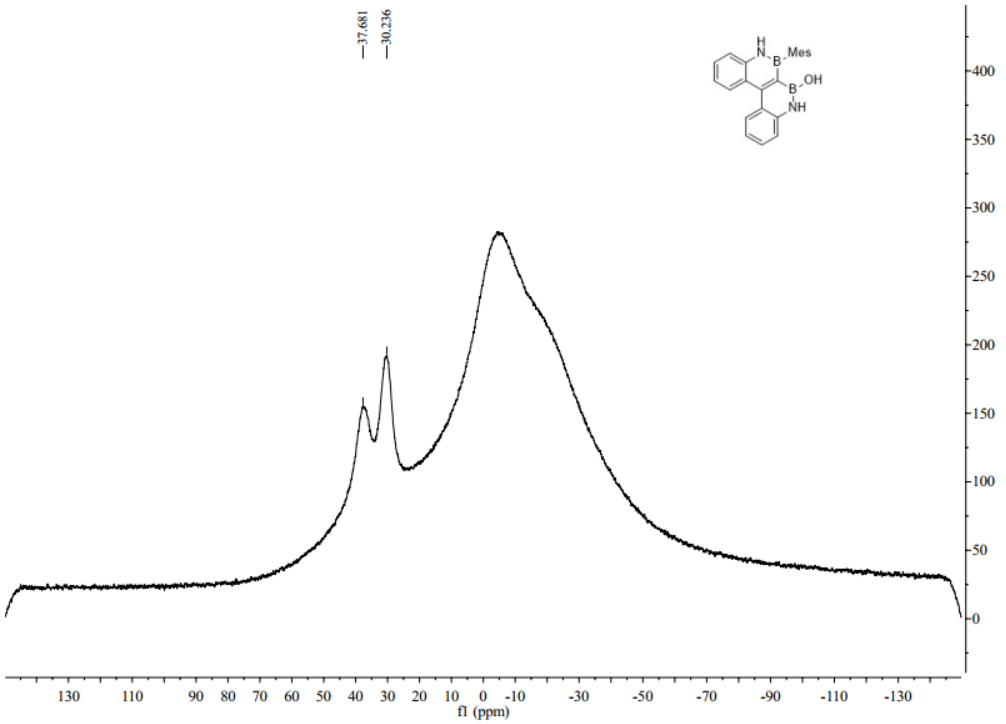

^{11}B NMR spectra of **4c** (128 MHz, $CDCl_3$). ^{11}B NMR chemical shifts are reported in ppm relative to external $BF_3{\cdot}OEt_2$ (0 ppm).

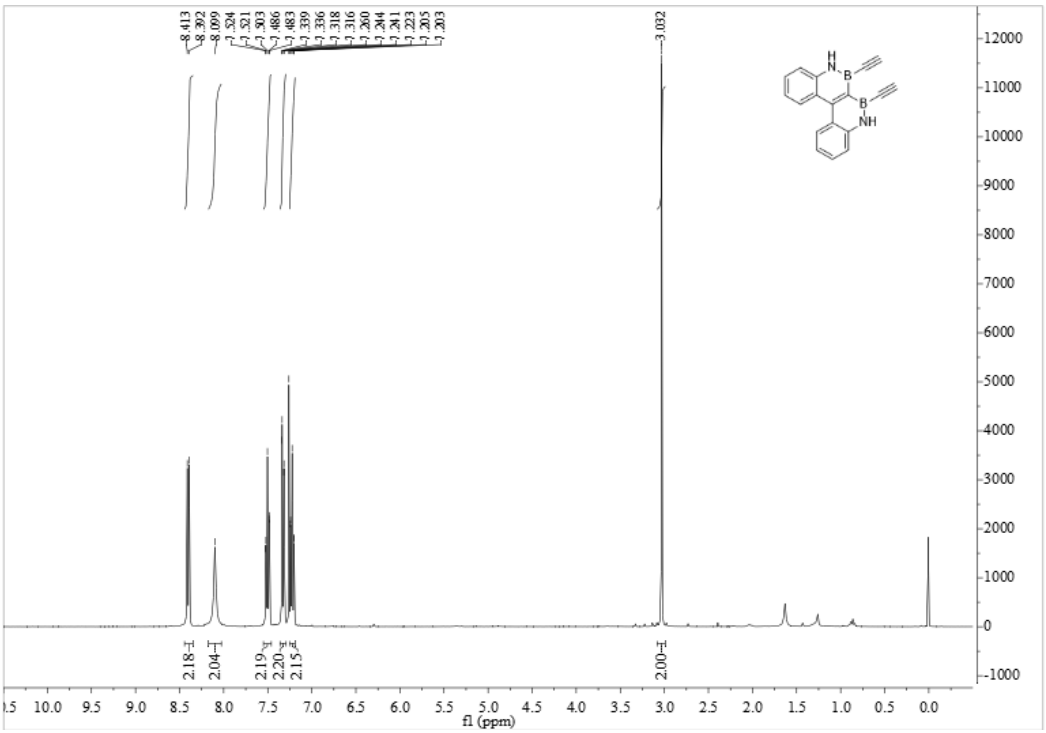

^{1}H NMR spectra of **4d** (400 MHz, $CDCl_3$)

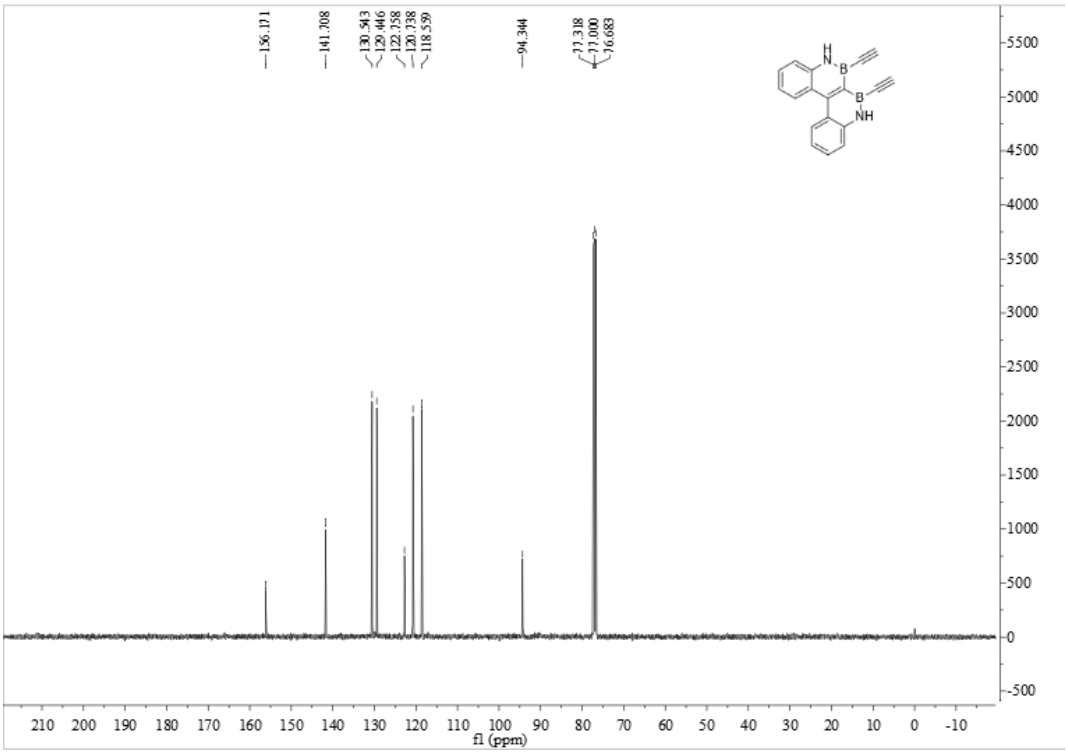

^{13}C NMR spectra of **4d** (100 MHz, $CDCl_3$)

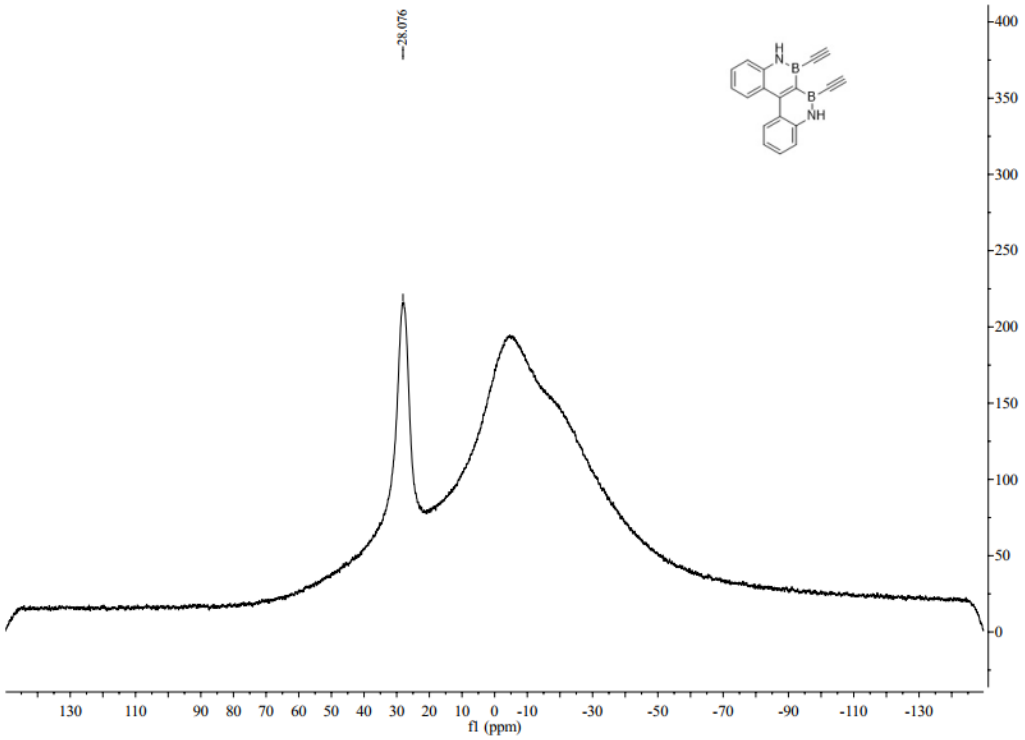

^{11}B NMR spectra of **4d** (128 MHz, $CDCl_3$). ^{11}B NMR chemical shifts are reported in ppm relative to external $BF_3{\cdot}OEt_2$ (0 ppm).

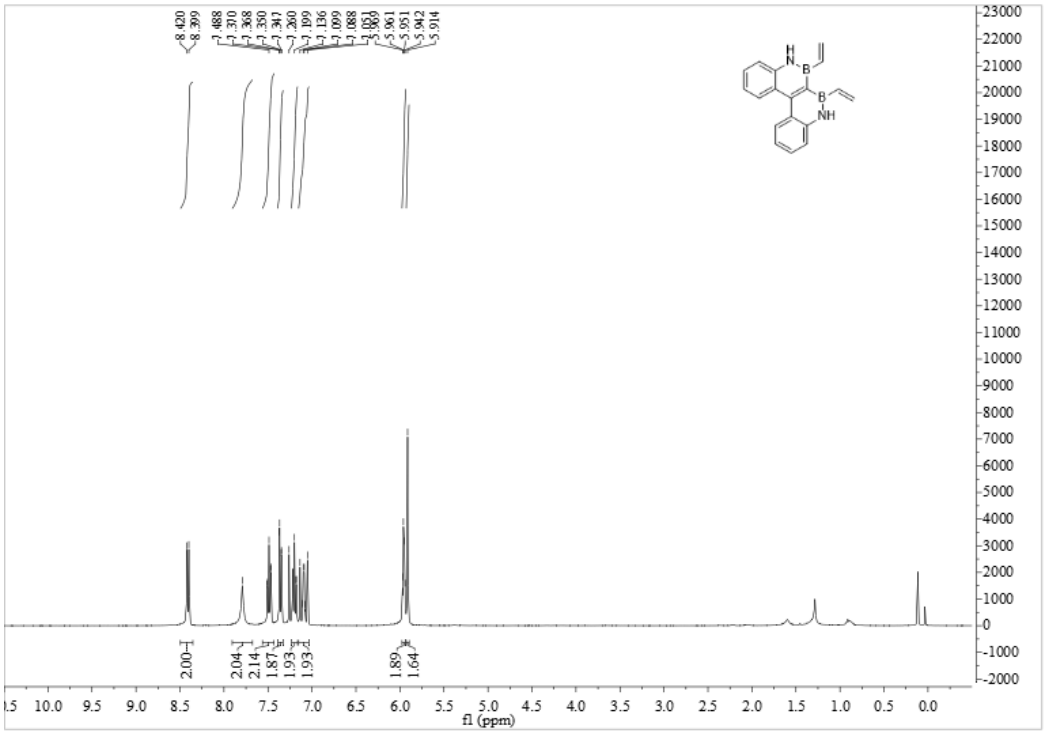

^{1}H NMR spectra of **4e** (400 MHz, $CDCl_3$)

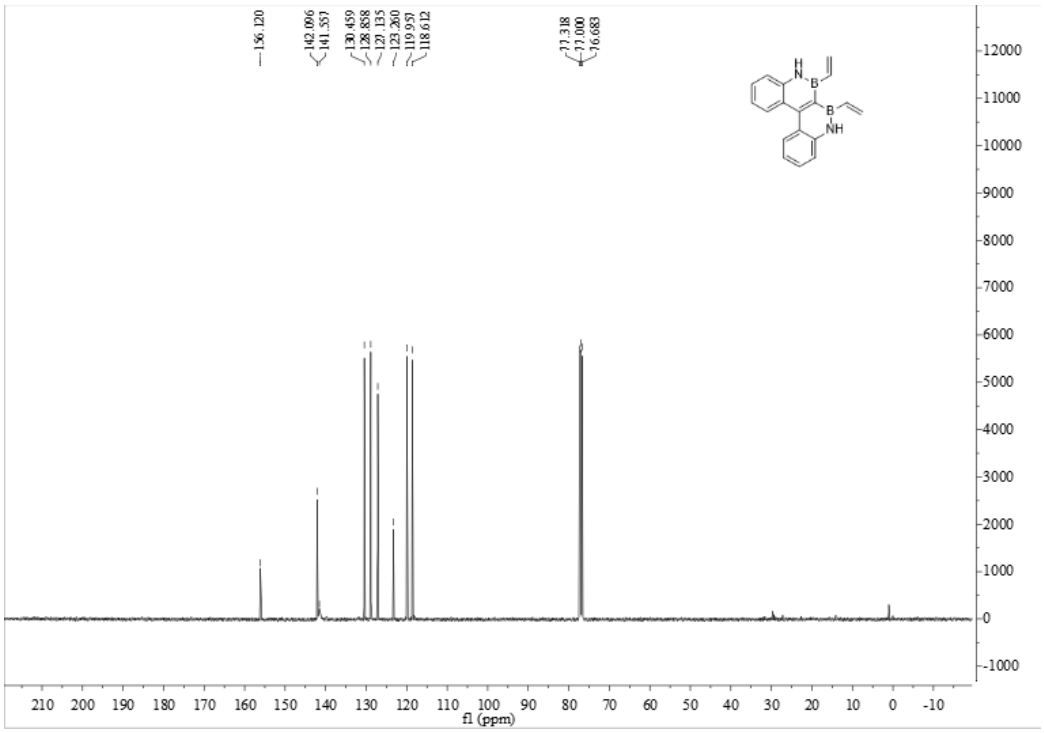

^{13}C NMR spectra of **4e** (100 MHz, $CDCl_3$)

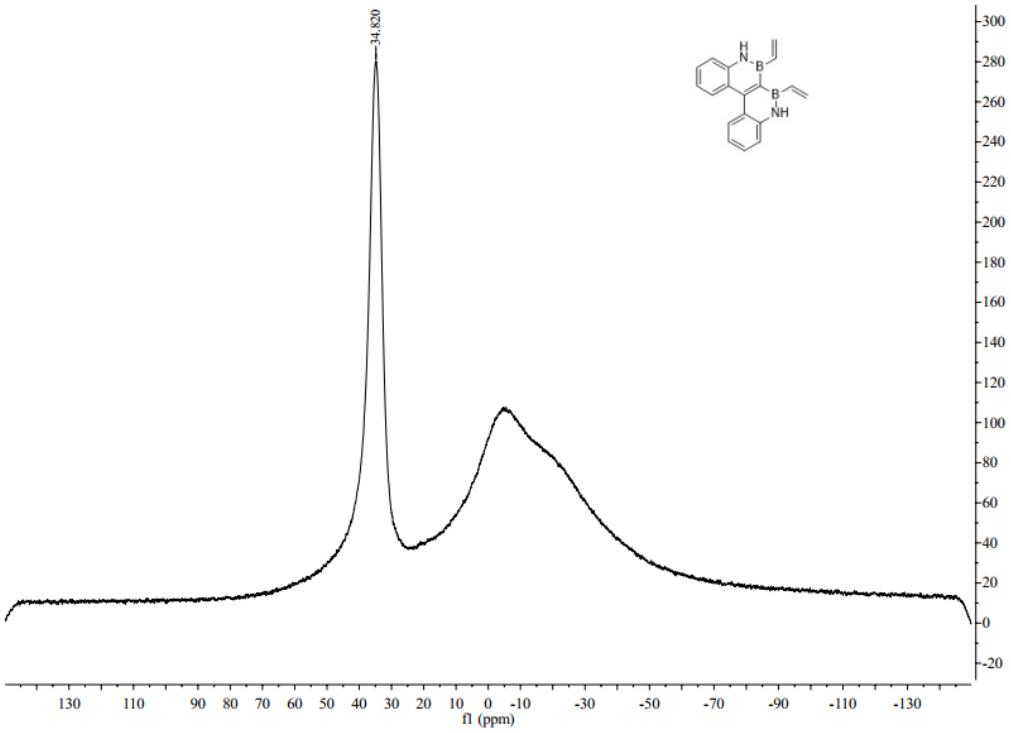

^{11}B NMR spectra of **4e** (128 MHz, $CDCl_3$). ^{11}B NMR chemical shifts are reported in ppm relative to external $BF_3{\cdot}OEt_2$ (0 ppm).

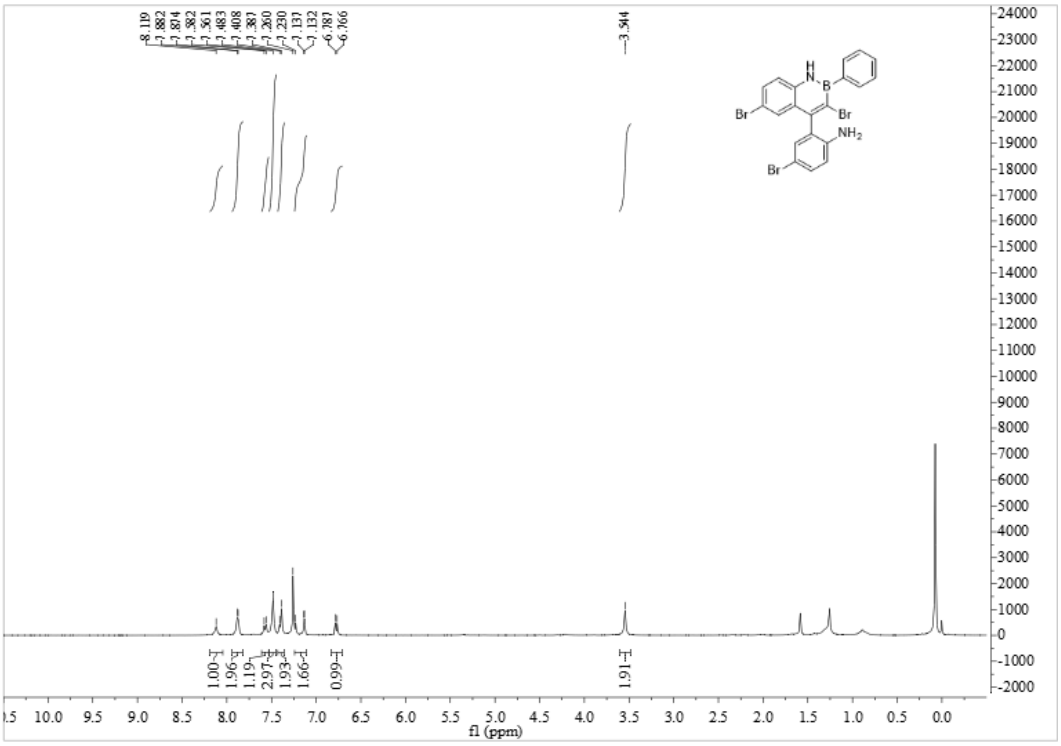

^{1}H NMR spectra of **5** (400 MHz, $CDCl_3$)

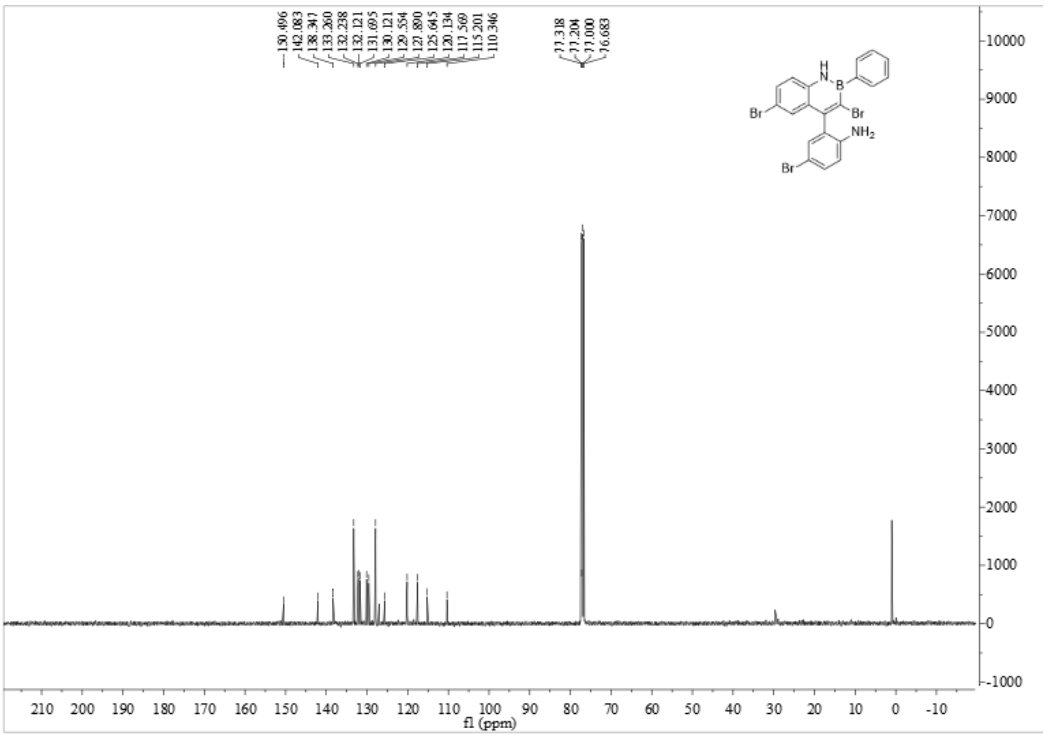

^{13}C NMR spectra of **5** (100 MHz, $CDCl_3$)

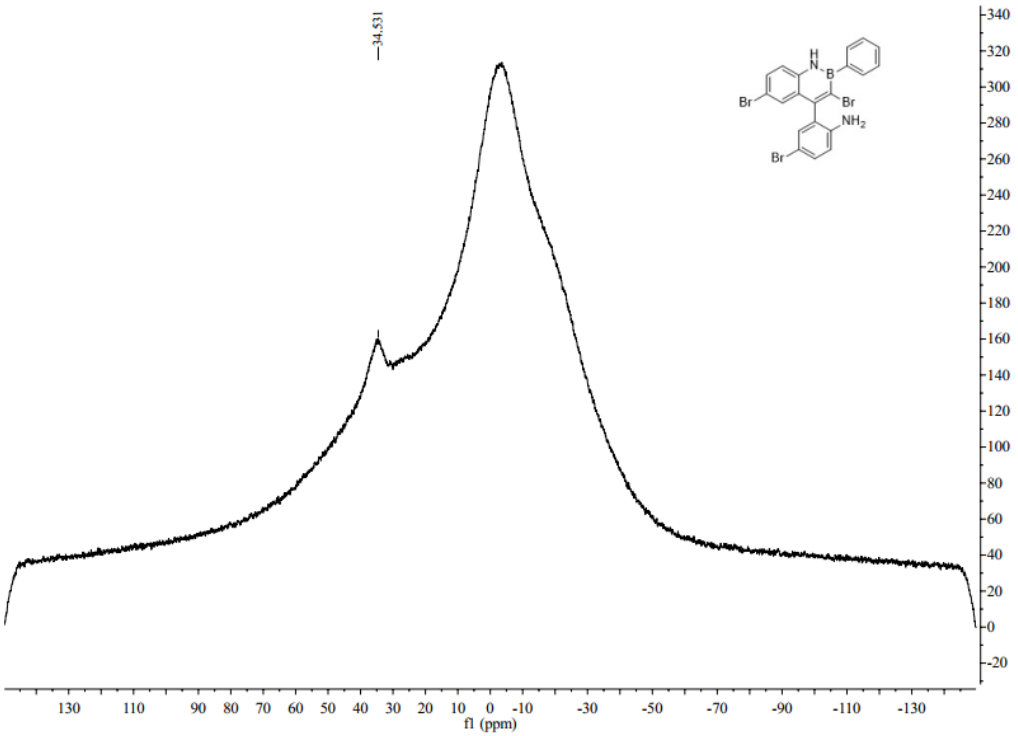

^{11}B NMR spectra of **5** (128 MHz, $CDCl_3$). ^{11}B NMR chemical shifts are reported in ppm relative to external $BF_3{\cdot}OEt_2$ (0 ppm).

8. References

[1] (a) Brouwer, A. M. *Pure Appl. Chem.*, **2011**, *83*, 2213-2228. (b) Meech, S.; Phillips, D. *J. Photochem.* **1983**, *23*, 193-217

[2] Lv, J.; Zhao, B.; Liu, L.; Han, Y.; Yuan, Y.; Shi, Z. *Adv. Synth. Catal*. **2018**, *360*, 4054-4059.

[3] (a) Abengozar, A.; Sucunza, D.; García-García, P.; Sampedro, D.; Perez-Redondo, A.; Vaquero, J. J. *Org. Lett*. **2019**, *21*, 2550-2554. (b) Abengozar, A.; Sucunza, D.; García-García, P.; Sampedro, D.; Perez-Redondo, A.; Vaquero, J. J. *J. Org. Chem*. **2019**, *84*, 7113-7122.

[4] Frisch, M. J.; Trucks, G. W.; Schlegel, H. B.; Scuseria, G. E.; Robb, M. A.; Cheeseman, J. R.; Scalmani, G.; Barone, V.; Mennucci, B.; Petersson, G. A.; Nakatsuji, H.; Caricato, M.; Li, X.; Hratchian, H. P.; Izmaylov, A. F.; Bloino, J.; Zheng, G.; Sonnenberg, J. L.; Hada, M.; Ehara, M.; Toyota, K.; Fukuda, R.; Hasegawa, J.; Ishida, M.; Nakajima, T.; Honda, Y.; Kitao, O.; Nakai, H.; Vreven, T.; Montgomery, J. A., Jr.; Peralta, J. E.; Ogliaro, F.; Bearpark, M.; Heyd, J. J.; Brothers, E.; Kudin, K. N.; Staroverov, V. N.; Kobayashi, R.; Normand, J.; Raghavachari, K.; Rendell, A.; Burant, J. C.; Iyengar, S. S.; Tomasi, J.; Cossi, M.; Rega, N.; Millam, J. M.; Klene, M.; Knox, J. E.; Cross, J. B.; Bakken, V.; Adamo, C.; Jaramillo, J.; Gomperts, R.; Stratmann, R. E.; Yazyev, O.; Austin, A. J.; Cammi, R.; Pomelli, C.; Ochterski, J. W.; Martin, R. L.; Morokuma, K.; Zakrzewski, V. G.; Voth, G. A.; Salvador, P.; Dannenberg, J. J.; Dapprich, S.; Daniels, A. D.; Farkas, O.; Foresman, J. B.; Ortiz, J. V.; Cioslowski, J.; Fox, D. J. *Gaussian 09, Revision A.02*; Gaussian, Inc., Wallingford, CT, **2009**.

[5] Becke, A. D. *J. Chem. Phys.* **1993**, *98*, 5648-5652.

[6] Scalmani, G.; Frisch, M. J. *J. Chem. Phys.* **2010**, *132*, 114110-114124.

[7] (a) Becke, A. D. Density-functional thermochemistry. III. The role of exact exchange. *J. Chem. Phys.,* **1993**, *98*, 5648-5652. (b) Lu, T.; Chen, F. Multiwfn: a multifunctional wavefunction analyzer. *J. Comput. Chem.* **2012**, *33*, 580-592.

[8] Liu, B.; Zhang, Y.; Chen, Y.; Liu, X.; Zhang L. Synthesis, Characterization and Photophysical Properties of BN-[4]helicenes. *Chin. J. Org. Chem*., 2020, **40**, 2879-2887.